

ABC of K_d Accuracy

Tong Ye Wang,^{1,2} Jean-Luc Rukundo,^{1,2} Zhiyuan Mao,^{1,2} Sergey N. Krylov*,^{1,2}

¹Department of Chemistry, York University, Toronto, Ontario M3J 1P3, Canada

²Centre for Research on Biomolecular Interactions, York University, Toronto, Ontario M3J 1P3, Canada

*Corresponding author's email: skrylov@yorku.ca

ABSTRACT: The equilibrium dissociation constant (K_d) is a major characteristic of affinity complexes and one of the most frequently determined physicochemical parameters. Despite its significance, the values of K_d obtained for the same complex under similar conditions often exhibit considerable discrepancies and sometimes vary by orders of magnitude. These inconsistencies highlight the susceptibility of K_d determination to large systematic errors, ultimately leading to misconceptions and significant misallocation of research and development resources. It is imperative to both minimize and quantitatively assess the systematic errors inherent in K_d determination. Traditionally, K_d values are determined through nonlinear regression of binding isotherms. This analysis utilizes three variables: concentrations of two reactants and a fraction R of unbound limiting reactant. The systematic errors in K_d arise directly from systematic errors in these variables. In this study, we thoroughly analyze the sources of systematic errors within these variables, aiming to mitigate their impact on K_d accuracy. Through this analysis, we illustrate how each source contributes to inaccuracies in K_d determination. Additionally, we propose a method for quantitatively assessing the confidence interval of systematic errors in concentrations, a crucial step towards quantitatively evaluating K_d accuracy. While presenting original findings, this paper also reiterates the fundamentals of K_d determination, hence, guiding researchers across all proficiency levels. By shedding light on the sources of systematic errors and offering strategies for their mitigation, our work will help researchers to enhance the accuracy of K_d determination thereby making binding studies more reliable.

1. Introduction

K_d values of affinity complexes drive important decisions, such as, ranking drug leads and choosing prevailing mechanisms in cellular regulation.¹⁻⁵ Correct decisions require accurate K_d values, but K_d values determined for the same complex under similar conditions often differ from each other by folds or even orders of magnitude while having small relative standard deviations.^{6,7} Such large differences suggest that K_d determination is subject to large systematic errors, or in other words, is inherently inaccurate. Systematic errors cannot be reduced by repeating the experiment multiple times. Inaccurate K_d values can lead to wrong ranking orders of drug leads and, as a result, disregarding high-potency hits while advancing low-potency ones.⁷⁻¹¹ Such mistakes inevitably lower the effectiveness of R&D efforts in drug development. Inaccurate K_d values can also lead to misinterpretation of biological results and fundamental misconceptions derailing fundamental biological research for long times.^{7, 12, 13} We emphasize that K_d values must be determined accurately, but this is often not the case. The problem is further aggravated by the lack of a method for quantitative assessment of K_d accuracy.

A classic way to determine K_d includes two major steps (Figure 1A).¹⁴⁻¹⁷ Step 1 is experimentally building a binding isotherm using a set of equilibrium mixtures containing two components: a limiting component, which we term ligand (L), and an excess component, which we term target (T). The ligand is kept at a constant total concentration L_0 across all while the total concentration of the target T_0 is varied from equilibrium mixture to equilibrium mixture in a wide range. A binding isotherm is the dependence of a fraction R of unbound (or bound) ligand on T_0 at a constant L_0 .

Step 2 in K_d determination is nonlinear regression of the binding isotherm with a known regression model, $R = F(L_0, T_0, K_d)$, derived from the definitions of R and K_d as well as mass balance for ligand, target, and complex. In this regression procedure, K_d is an unknown sought parameter, L_0 and T_0 are known independent variables, and R is a known dependent variable. The result of nonlinear regression is a determined K_d value ($K_{d,det}$) and its standard deviation σ obtained under the assumption that all three variables (L_0 , T_0 , and R) are subject to random errors only. The value of σ describes the precision of $K_{d,det}$ and suggests nothing about the accuracy of $K_{d,det}$.^{18, 19} In other words, the probability of accurate K_d to be found inside of the $K_{d,det} \pm \sigma$ range is unknown and can be very low.

As K_d is not measured directly, but determined using nonlinear

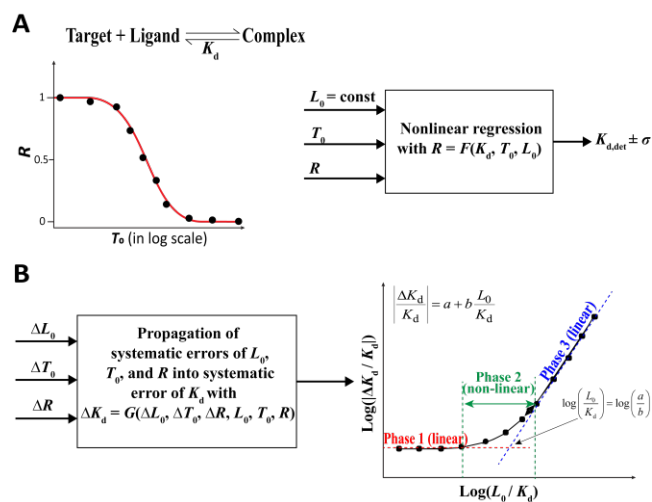


Figure 1. Schematic representations of **A)** determination of K_d and its standard deviation (σ) by nonlinear regression with three variables from the binding isotherm (L_0 , T_0 , and R) and **B)** propagation of systematic errors in these variables leading to a triphasic dependence of the relative systematic error in K_d on the ratio L_0/K_d in which K_d designates its true unknown value.²⁰

regression with a known regression model, the accuracy of K_d is defined by the accuracy of the three variables (L_0 , T_0 , and R) (Figure 1B). Using error propagation rules, we can link the systematic error in K_d to systematic errors in L_0 , T_0 , and R : $\Delta K_d = G(\Delta L_0, \Delta T_0, \Delta R, L_0, T_0, R)$. The dependence of ΔK_d on L_0 is such that when L_0 is much greater than the unknown true value of K_d , then the relative systematic error in K_d is equal to a combination of relative systematic errors in the variable multiplied by L_0/K_d (where K_d is its unknown true value).²⁰ Decreasing systematic errors in K_d thus requires decreasing both L_0 and systematic errors in the variables. As decreasing L_0 is restricted by limits of quantitation (LOQ) of instruments, decreasing systematic errors in variables is viewed as an effective way of improving the accuracy of K_d determination.

Minimizing the systematic error in K_d is an important task which can be translated into minimizing systematic errors in the variables. The drawback of such minimization is that it is blind; we minimize the error without knowing its value. The limitation of blind minimization is that even if all known precautions are taken

to minimize systematic errors in variables (and, thus, in K_d), the resulting $K_{d,\text{det}}$ may still be not sufficiently accurate for an intended application, but we will not know that. The major problem, which is not directly addressed in this work, is the lack of an approach for quantitative assessment of K_d accuracy. We view the understanding of error propagation (Figure 1B) as an important starting point in the development of such an approach. The prospective approach for quantitative assessment of K_d accuracy requires more than just the minimization of systematic errors in variables; it requires their quantitative assessment. Thus, we started the presented work with two goals in mind: (i) minimization of systematic errors in variables and (ii) quantitative assessment of these errors for the prospective approach of quantitative assessment of the accuracy of K_d . Accordingly, after providing the required theoretical background on K_d determination and error propagation, we analyze major sources of systematic errors in variables R , L_0 , and T_0 , and we also identify means of minimizing these errors and study how they can be quantitatively assessed. Below, we outline the structure of this paper.

We start with analyzing sources of systematic errors in R and their influence on the accuracy of $K_{d,\text{det}}$. We uncover that the first and arguably most obvious source of systematic errors in R – a mistaken use of non-additive signals – is widely neglected. For example, light polarization is a non-additive signal when applied to fluorescence since it cannot be directly decomposed into the sum of signals contributed by the target-unbound and target-bound ligands.^{21,22} However, non-additive polarization is commonly used instead of additive anisotropy in fluorescence-based K_d determination, and it is often built-in as a default output signal in commercial instrumentation.²³⁻²⁷ The second common source of systematic errors in R is inadequate instrument calibration and incorrectly determined calibration parameters, such as quantum yields when using fluorescence intensity as signal and the grating factor G when using anisotropy as signal. The third source of systematic errors in R is not reaching equilibrium in the binding reaction or saturation in the binding isotherm. We demonstrate that all these qualitatively-distinct sources of systematic errors in R can cause gross systematic errors in $K_{d,\text{det}}$, especially for large values of L_0/K_d .

To help researchers minimize systematic errors in R , we (i) provide a comprehensive list of signals used in calculating R values, with information on signal additivity, (ii) discuss in detail how to increase the accuracies of calibration parameters, and (iii) suggest quantitative guidance for reaching equilibrium and saturation. When the systematic error of R is minimized, its range can be roughly estimated by experienced experimentalists, but this estimate can hardly be used in the accuracy assessment of $K_{d,\text{det}}$. Unfortunately, our current results do not suggest a rational and general approach for quantitatively assessing the systematic error of R .

Then, we analyze sources of systematic errors in concentrations L_0 and T_0 . The first and most well-known source of systematic errors in concentrations is uncalibrated measuring equipment (if concentrations are calculated based on the weight of solid material and volume of solvent) or an uncalibrated spectrophotometer (if concentrations are calculated using spectrophotometry, i.e., the Lambert-Beer law). Additionally, if concentrations are calculated using the Lambert-Beer law, systematic errors in molar extinction coefficients can also lead to systematic errors in concentrations. The second common source of systematic errors in L_0 and T_0 is impurities in reagents. The third source is solute adsorption to surfaces of vials, channels, etc. We quantitatively demonstrate that all these sources of inaccuracies of concentrations have similar and severe effects on the accuracy of $K_{d,\text{det}}$. The systematic errors in concentrations caused by the common sources can be minimized by proper optimization of experimental methods. To assist experimentalists in minimizing systematic errors in L_0 and T_0 , we (i) list the common procedures of calibrating measuring equipment and rules for operating the equipment correctly, (ii) suggest

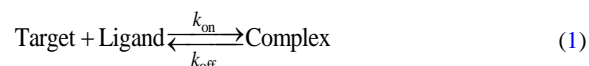
approaches to determining the purity of reagents, and (iii) discuss measures for reducing solute adsorptions to surfaces. At last, we also provide a checklist of measures to be undertaken when designing experiments to avoid common mistakes and minimize systematic errors in R , L_0 and T_0 .

Systematic errors in concentrations can be largely reduced with cautious method optimization but, like any other systematic errors, they cannot be fully eliminated. In K_d -determination with nonlinear regression, the unavoidable systematic errors in L_0 and T_0 are from random errors in the concentration of stock solutions used to prepare other solutions. Since the random error in the concentration of a stock solution is normally distributed (in an infinite number of stock solution preparations), the confidence interval of systematic error in the concentration of a diluted solution (i.e., L_0 or T_0) can be quantitatively assessed by measuring the random error in concentrations of multiple stock solutions prepared from scratch. Combined with error propagation (Figure 1B), the approach of determining confidence intervals of the errors in L_0 and T_0 sets a cornerstone for finding confidence intervals of accurate K_d in the future.

2. Theoretical Background

2.1. Binding Reaction

We consider a 1:1 binding reaction between a target and a ligand:



where k_{on} and k_{off} are rate constants of complex formation and dissociation, respectively. K_d can be defined through either these rate constants or equilibrium concentrations of the target (T), ligand (L), and complex (C), as follows:

$$K_d = \frac{k_{\text{off}}}{k_{\text{on}}} = \frac{TL}{C} \quad (2)$$

Lower K_d values correspond to higher complex stability. The equilibrium concentrations are linked to each other through the formal total concentrations of the target (T_0) and ligand (L_0) according to the rules of mass balance:

$$T_0 = T + C, \quad L_0 = L + C \quad (3)$$

T_0 and L_0 are concentrations of target and ligand, respectively, after mixing solutions of these two reactants but before any complex is formed. Experimentally, T , L , and C cannot be directly measured to determine the K_d . However, K_d can be calculated with known T_0 , L_0 , and fraction of unbound ligand R ; the latter links K_d to T_0 and L_0 .

2.2. Fraction R of Unbound Ligand

The determination of K_d requires experimentally finding a fraction R of target-unbound ligand (or a fraction of target-bound ligand, $1 - R$), in the equilibrium mixture of the target and ligand:

$$R = \frac{L}{L_0} \quad (4)$$

The general procedure for finding R starts with preparing the equilibrium mixture of the ligand and target. The procedure is facilitated by the physical or spectral separation of the unbound ligands from the complex. The separation is complete if the peaks or spectra of the unbound ligand and the complex do not overlap; otherwise, it is incomplete. The choice of a signal-processing approach depends on whether or not the separation is complete.

Complete separation of the unbound ligand from the target-ligand complex allows one to measure two signals from the equilibrium mixture: one is a signal from the unbound ligand (S_L) and the other is a signal from the target-ligand complex (S_C), and express R using the two signals:^{16, 28, 29}

$$R = \frac{L}{L_0} = \frac{S_L}{S_L + S_C/\varphi} \quad (5)$$

where φ is a factor by which the signal of ligand changes when it binds the target, e.g., in the case of fluorescence detection, φ is the quantum yield of the target-bound ligand relative to that of the unbound ligand.

Only a cumulative signal S from the unbound ligand and the target-bound ligand in the equilibrium mixture can be measured when their separation is incomplete. Typically, R is determined using additive signals (signal additivity is explained in detail in [Note S1](#)), which satisfy the principle of superposition:^{15, 17, 30, 31}

$$S = S_L^* \frac{L}{L_0} + S_C^* \frac{C}{L_0} \quad (6)$$

where S_L^* and S_C^* are signals from equimolar concentrations of pure ligand and pure complex and S is a signal from a mixture containing both unbound ligand and complex of a total concentration equal to that used to measure S_L^* and S_C^* . Note that, signal being linearly dependent on concentration is a sufficient condition for the establishment of [Eq 6 \(Note S2\)](#). In the case of incomplete separation of signals from the unbound and target-bound signals, the value of R can still be determined, but three signals, S , S_C^* , and S_L^* , are required instead of two signals in [eq 5](#):^{15, 17, 30, 32}

$$R = \frac{S - S_C^*}{S_L^* - S_C^*} \quad (7)$$

Measuring signal S for the mixture is trivial. Measuring signal S_L^* for pure ligand is also trivial as S_L^* is the signal from the ligand in the absence of target. Measuring signal S_C^* from the pure complex in the case of incomplete separation requires that $C \gg L$ which is achieved *via* using a saturating total concentration of the target in the equilibrium mixture:

$$T_0 > L_0, \quad T_0 \gg K_d \quad (8)$$

Target solubility and a significant increase in viscosity of the sample due to excessively high T_0 may limit the ability to find S_C^* . Accordingly, complete separation of the free and target-bound ligands is preferable to incomplete separation.

2.3. General Approach to K_d Determination

There are two major approaches for finding K_d when R has been determined. In the first approach, a formula that explicitly relates K_d to R is used:³³

$$K_d = \frac{T_0 - L_0(1-R)}{(1/R-1)} \quad (9)$$

This formula is obtained by solving [eq 2](#) using mass balance equations for both ligand and target ([eq 3](#)), and the definition of R ([eq 4](#)). This approach requires a single value of R . Calculation of K_d with this formula is most accurate for R approximately equal to $1/2$.¹⁶ However, K_d values determined this way are very sensitive to random errors of R , T_0 , and L_0 , especially when R is closer to zero or unity than to $1/2$ ([Note S3](#)). Therefore, an alternative approach, which relies on nonlinear regression is typically used.

In the nonlinear-regression approach, K_d is determined by using multiple values of R found for a constant value of L_0 but different values of T_0 . The dependence of R on T_0 is called a binding isotherm, which exhibits a characteristic sigmoidal shape in a semilogarithmic presentation of the isotherm (dots in [Figure 1](#)). K_d is then computed by fitting the binding isotherm with a theoretical dependence of R on T_0 :^{16, 17, 34}

$$R = -\frac{K_d + T_0 - L_0}{2L_0} + \sqrt{\left(\frac{K_d + T_0 - L_0}{2L_0}\right)^2 + \frac{K_d}{L_0}} \quad (10)$$

while using K_d as a fitting parameter, i.e., K_d is varied to obtain the best fit ([eq 10](#) can be obtained by solving [eq 9](#) for R). An example of the best fit of a binding isotherm is shown as a red line in

[Figure 1](#). In the nonlinear-regression procedure, K_d is a determined parameter, L_0 and T_0 are independent variables and R is a dependent variable.

The regression model presented by [eq 10](#) assumes that only random errors are present in R , T_0 , and L_0 . Those errors result in a random error of $K_{d,det}$ which is reported at the output of nonlinear regression as a standard deviation σ . The standard deviation (σ) of $K_{d,det}$ along with the mean value of $K_{d,det}$ indicates the precision of $K_{d,det}$. Importantly, it is not necessary to repeat the determination of R for the same value of T_0 to assess the random error of $K_{d,det}$.

If any of R , T_0 , or L_0 has a systematic error, then K_d cannot be determined accurately with a model presented by [eq 10](#). Furthermore, if systematic errors exist in R , T_0 , or L_0 and their magnitudes are unknown, then not only is $K_{d,det}$ inaccurate, but also the systematic error in $K_{d,det}$ remains unknown. On the other hand, if some information about the accuracy of R , T_0 , or L_0 is known then the correct regression model presented by [eq 10](#) can help assess the accuracy of K_d .

2.4. Propagation of Systematic Errors

The accuracy of $K_{d,det}$ depends on the accuracies of L_0 , T_0 and R . If the values of L_0 , T_0 and R were known accurately (i.e., had no systematic errors), then K_d determination would be accurate (e.g., subject to random errors only). However, this is not the case, and systematic errors in L_0 , T_0 , and R (designated as ΔL_0 , ΔT_0 , and ΔR) translate to the systematic error in K_d (designated as ΔK_d) as explained below assuming (for now) that ΔL_0 , ΔT_0 , and ΔR are known.

The manner in which ΔL_0 , ΔT_0 , and ΔR are translated into ΔK_d is governed by the error-propagation rules. Such rules, in turn, depend (though not critically) on whether ΔL_0 , ΔT_0 , and ΔR are strongly or weakly correlated. If they are strongly correlated (which will be the case if similar procedures are used for the preparation of solutions of ligand and target, and ΔR is solely the consequence of ΔL_0 and ΔT_0), then we can approximate the absolute value of ΔK_d by the following expression based on the using of error propagation rule for fully correlated errors:

$$|\Delta K_d| = \left| \left(\frac{\partial K_d}{\partial T_0} \right) \Delta T_0 \right| + \left| \left(\frac{\partial K_d}{\partial L_0} \right) \Delta L_0 \right| + \left| \left(\frac{\partial K_d}{\partial R} \right) \Delta R \right| \quad (11)$$

We can apply [eq 11](#) to the dependence of K_d on L_0 , T_0 , and R ([eq 9](#)) and obtain:²⁰

$$\left| \frac{\Delta K_d}{K_d} \right| = a + b \frac{L_0}{K_d} \quad (12)$$

where a is a constant depending only on $|\Delta T_0/T_0|$ and $|\Delta R/R|$ while b is a constant depending on all three relative errors: $|\Delta T_0/T_0|$, $|\Delta L_0/L_0|$ and $|\Delta R/R|$.

If ΔL_0 , ΔT_0 , and ΔR are weakly correlated (which will be the case if different procedures are used for the preparation of solutions of ligand and target, and ΔR is independent of ΔL_0 and ΔT_0), then we can approximate the absolute value of ΔK_d by the following expression based on the use of error propagation rule for fully uncorrelated errors:

$$|\Delta K_d| = \sqrt{\left(\frac{\partial K_d}{\partial T_0} \right)^2 \Delta T_0^2 + \left(\frac{\partial K_d}{\partial L_0} \right)^2 \Delta L_0^2 + \left(\frac{\partial K_d}{\partial R} \right)^2 \Delta R^2} \quad (13)$$

We can apply [eq 13](#) to the dependence of K_d on L_0 , T_0 , and R ([eq 9](#)) and obtain:²⁰

$$\left| \frac{\Delta K_d}{K_d} \right| = \sqrt{\alpha^2 + \lambda \frac{L_0}{K_d} + \beta^2 \left(\frac{L_0}{K_d} \right)^2} \quad (14)$$

where α and λ are constants depending only on $|\Delta T_0/T_0|$ and $|\Delta R/R|$ while β is a constant depending on all three relative errors: $|\Delta T_0/T_0|$, $|\Delta L_0/L_0|$ and $|\Delta R/R|$. In propagating the errors to obtain [eqs 12](#) and [14](#), a single simplifying assumption was made, that the determined (from measured signals) value of R is equal to 0.5, which leads to

the least erroneous $K_{d,\text{det}}$.^{16, 20} Thus, we are considering the best-case scenario and eqs 12 and 14 represent the lower limit for relative systematic errors in K_d . Exact dependencies of a and b as well as α , λ , and β on $|\Delta T_0/T_0|$, $|\Delta L_0/L_0|$, and $|\Delta R/R|$ are not important here but can be found elsewhere.²⁰

Although eqs 12 and 14 appear different, they are similar in the triphasic shape of $|\Delta K_d/K_d|$ dependence on L_0/K_d (Figure 1B). The first phase corresponds to low L_0/K_d values and is linear with negligible dependence of $|\Delta K_d/K_d|$ on L_0/K_d . The reason for the first phase to be virtually parallel to the x -axis is that the first term prevails over the second in eq 12 and the first two terms prevail over the third term in eq 14 for low values of L_0/K_d . For phase 3, which corresponds to large L_0/K_d values, eqs 12 and 14 approach another linear phase: $|\Delta K_d/K_d| = b(L_0/K_d)$ and $|\Delta K_d/K_d| = \beta(L_0/K_d)$, respectively; that phase shows a high sensitivity of $|\Delta K_d/K_d|$ to L_0/K_d . There is a non-linear transition range (phase 2) between the two linear phases. Moreover, both eqs 12 and 14 suggest that the minimum $|\Delta K_d/K_d|$ value depends on a single parameter (a in eq 12 or α in eq 14) that is defined only by $|\Delta T_0/T_0|$ and $|\Delta R/R|$, while the sensitivity of $|\Delta K_d/K_d|$ to L_0/K_d in phase 3 mainly depends on a parameter (b in eq 12 or β in eq 14) that is defined by relative errors of all three variables: $|\Delta T_0/T_0|$, $|\Delta L_0/L_0|$, and $|\Delta R/R|$.

As suggested by eqs 12 and 14, to increase the accuracy of $K_{d,\text{det}}$ (i.e., to decrease $|\Delta K_d/K_d|$), one can decrease the ligand concentration L_0 (to reduce L_0/K_d ratio) and/or minimize the relative systematic errors in L_0 , T_0 , and R . Since L_0 cannot be lower than LOQ of an instrument utilized for measuring signals (and, thus, finding the values of R),²⁰ it is not practical to decrease L_0/K_d to a very low value in many cases, especially in the studies of very stable complexes (small K_d values). Thus, understanding the sources of systematic errors in L_0 , T_0 , and R and how these errors influence the accuracy of K_d is crucial for minimizing such systematic errors and further improving the accuracy of K_d .

3. Results and Discussion

3.1. Sources of Systematic Errors in R

Systematic errors in $K_{d,\text{det}}$ can be attributed to systematic errors in R , which can originate from various sources. Here, we analyze four common sources of ΔR , which are: (i) using non-additive signals to calculate R , (ii) uncalibrated signal-detection instrument or using incorrectly determined calibration parameters in calculating R (iii) the insufficient incubation time for mixtures not reaching equilibrium, and (iv) measuring Sc^* (signal for pure complex) without satisfying saturation condition described in eq 8. Most of these error sources result from theoretical or experimental

mistakes and should be addressed during the experimental design and preliminary experiments.

3.1.1. Non-Additive Signals

Systematic errors in R can arise from the use of a non-additive signal, which does not satisfy eq 6 and, accordingly, cannot be used in eq 7 (derived from eq 6) to calculate R . Examples of K_d -determination approaches using signals that have been proven to be additive/non-additive are shown in Table 1. In addition, some examples of approaches using signals whose additive characters (to our best knowledge) have not been proven are also shown in Table 1 with question marks (?) in the column of "Additivity". Table 1 serves as a starting point for reviewing the additive characters of the signals used in various K_d -determination approaches. Researchers in the field of K_d determination are invited to supplement and/or correct this information and publish an updated table on https://www.researchgate.net/post/Additivity_of_signals_used_in_equilibrium_Kd-determination_approaches. Here, considering examples of non-additive signals within the context of specific K_d -determination approaches is instructive. Our results indicate that a signal must be proven to be additive before it can be used to calculate R . Otherwise, large systematic errors in $K_{d,\text{det}}$ might be caused by mistakenly using non-additive signals in R calculations.

3.1.1.1. Mobility-Based Methods

A method commonly used for K_d determination for relatively unstable complexes is based on mobilities of unbound ligand and target-bound ligand in capillary electrophoresis (CE).³⁵ In this method, a short plug of the ligand of concentration L_0 is injected into a capillary prefilled with the running buffer containing the target at a concentration of T_0 . This plug of the ligand moves through the capillary by an electric field under the condition of pseudo-equilibrium in binding reaction (eq 1) which is equivalent to a condition that the characteristic equilibration time (t_{eq}) is much smaller than the characteristic separation time (t_{sep}):

$$t_{\text{eq}} \ll t_{\text{sep}} \quad (15)$$

The characteristic equilibration time for a case of $T_0 \gg L_0$ can be approximated by:³⁶

$$t_{\text{eq}} \approx (k_{\text{off}} + k_{\text{on}}T_0)^{-1} \quad (16)$$

The characteristic separation time is:

$$t_{\text{sep}} = \frac{l}{\min(|v_T - v_L|, |v_C - v_L|)} \quad (17)$$

where l is the length of the plug of ligand, and v_T , v_L , and v_C are

Table 1. Examples of K_d -determination approaches and the additive characters of the signals used to calculate R .

Approach	Signal	Additivity	Ref
Accurate Constant <i>via</i> Transient Incomplete Separation (ACTIS)	Fluorescence or ion signal intensities	Yes	[17], [56], [57]
Affinity Capillary Electrophoresis (ACE)	Mobility or migration velocity	Yes	[35], [38], [39]
Back-scattering Interferometry (BSI)	Refractive index in solution	?	[94]
Biolayer Interferometry (BLI)	Wavelength shift	Yes	[95]
Enzyme-Linked Immunosorbent Assays (ELISA)	Absorbance	Yes	[96]
Flow Induced Dispersion Analysis (FIDA)	Apparent diffusion coefficient	No	[44], [46]
Fluorescence Anisotropy (FA)	Anisotropy	Yes	[40]
Fluorescence Polarization (FP)	Polarization	No	[21–23]
Fluorescence Resonance Energy Transfer (FRET)	Fluorescence	Yes	[97]
High-Performance Liquid Chromatography (HPLC)	Migration velocity	Yes	[98], [99]
Isothermal Titration Calorimetry (ITC)	Enthalpy change	Yes	[100], [101]
Microscale Thermophoresis (MST)	Fluorescence	Yes	[15]
Nano-electrospray Ionization Mass Spectrometry (nESI-MS)	Ion signal intensities	Yes	[102], [103]
Nuclear Magnetic Resonance (NMR)	Chemical shift	Yes	[7]
Nuclear Magnetic Resonance (NMR)	Longitudinal and transverse relaxation rates	No	[7], [104]
Solid Phase Radioimmunoassay (SPRIA)	Radioactivity	?	[105]
Surface Plasmon Resonance (SPR)	Resonance angle	Yes	[88]
Taylor dispersion analysis (TDA)	Reciprocal of apparent diffusion coefficient	No	[106]

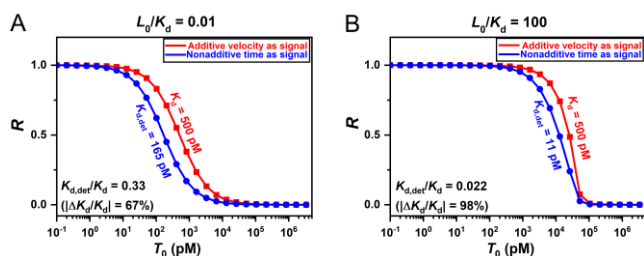


Figure 2. Comparison of the results produced by using the additive velocity (v) and non-additive time (t) as signals: binding isotherms and $K_{d,det}$ obtained with signals of velocity (red) and time (blue) for $L_0/K_d = 0.01$ (A) and $L_0/K_d = 100$ (B). In the simulation, the theoretical/input $K_d = 500$ pM.

velocities of the target, ligand, and complex, respectively. Usually, the complex moves with the velocity intermediate to those of the unbound ligand and target, that is $|v_C - v_L| < |v_T - v_L|$, and eq 17 can be written as:

$$t_{sep} = \frac{l}{|v_C - v_L|} \quad (18)$$

The migration time of the peak of ligand to the detector t is a common measurable signal in capillary electrophoresis (CE),³⁷ but time is not additive, while the velocity and inverse migration time are both additive:^{35, 38, 39}

$$v = v_L \frac{L}{L_0} + v_C \frac{C}{L_0} \quad (19)$$

$$\frac{1}{t} = \frac{1}{t_L} \frac{L}{L_0} + \frac{1}{t_C} \frac{C}{L_0}$$

Binding isotherms with both time and velocity as a signal have characteristic sigmoidal shapes; however, they are shifted with respect to each other (Figure 2). If one wrongly uses time instead of inverse time to calculate R with eq 7, then the resulting $K_{d,det}$ will have significant systematic errors at both low and high L_0/K_d values (Figure 2).

3.1.1.2. Methods Based of Fluorescence Anisotropy

Both fluorescence anisotropy (r) and polarization (P) are the parameters that quantitatively describe the degree of light polarization in different contexts.⁴⁰ Fluorescence anisotropy was introduced specifically to characterize light emitted by a fluorophore in three dimensions while polarization was introduced to characterize polarization of a beam of collimated light from a light source in a plane perpendicular to the beam. Thus, fluorescence anisotropy and beam-light polarization are applied to different dimensionalities which are reflected in formulas expressing r and P through the two component light intensities.

Fluorescence anisotropy is defined as follows:⁴⁰

$$r = \frac{I_{||} - I_{\perp}}{I_{||} + 2I_{\perp}} \quad (20)$$

where $I_{||}$ is the intensity of light emitted by a fluorophore with a polarization orientation parallel to that of the excitation light; I_{\perp} is the intensity of emitted light with a polarization orientation perpendicular to that of the excitation light. The denominator of eq 20 contains a factor of 2 because there are two symmetrical dimensions perpendicular to the direction of excitation-light polarization, but only the intensity associated with one of them (i.e., I_{\perp}) is typically measured. The denominator represents the total intensity of light in the three-dimensional space.

Beam-light polarization is defined as follows:⁴¹

$$P = \frac{I_{max} - I_{min}}{I_{max} + I_{min}} \quad (21)$$

where I_{max} is the intensity of light polarized in the direction which corresponds to maximum intensity; I_{min} is the intensity of light in

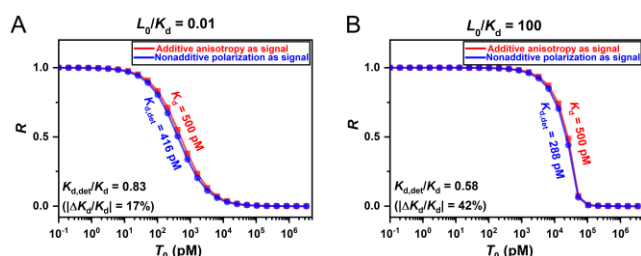


Figure 3. Comparison of the results produced by additive anisotropy (r) and non-additive polarization (P): binding isotherms and $K_{d,det}$ obtained with anisotropy (red) and polarization (blue) at $L_0/K_d = 0.01$ (A) and $L_0/K_d = 100$ (B). In the simulation, the theoretical/input $K_d = 500$ pM.

the direction perpendicular to the first one. The denominator also represents the total intensity of light but in two-dimensional space. Eq 21 is sometimes written using $I_{||}$ instead of I_{max} and I_{\perp} instead of I_{min} .⁴⁰

$$P = \frac{I_{||} - I_{\perp}}{I_{||} + I_{\perp}} \quad (22)$$

which is legitimate provided that we understand that P describes a two-dimensional case due to the missing factor of 2 in the denominator.

Formally, anisotropy and polarization calculated with eq 20 and eq 22, respectively, are closely related and interconvertible with:⁴⁰

$$r = \frac{2P}{3-P} \quad (23)$$

Anisotropy has been proven to be an additive signal:⁴²

$$r = r_L \frac{L}{L_0} + r_C \frac{C}{L_0} \quad (24)$$

and thus can be used to correctly calculate R with eq 7 and, then, build an accurate binding isotherm and accurately determine K_d with eq 10.²² However, by combining the interconversion formula (eq 23) and the proof of anisotropy additivity (eq 24), we can easily conclude that P is non-additive (Note S4) and, thus, cannot be directly used to calculate R . The non-additivity of P (without transformations) was explained decades ago,^{21, 22} but it is still mistakenly used instead of r in eq 7 for finding R and K_d determination.

Additionally, some commercial instruments provide polarization (P) as a default output,^{26, 27} which can mislead users into calculating R based on P . Such a mistake can only be explained by a widely spread ignorance, as replacing P with r is not only correct but also does not require any changes in instrument hardware.

When one uses the non-additive P instead of additive r to calculate R with eq 7, the binding isotherm will slightly shift due to the systematic errors introduced to R (Figure 3). Without including any other source of systematic errors, these small shifts of binding isotherm cause $< 20\%$ relative systematic error in $K_{d,det}$ for small L_0/K_d . However, the effect of this shift on the accuracy of $K_{d,det}$ grows with increasing L_0/K_d and may result in $> 40\%$ relative systematic errors for large L_0/K_d (Figure 3B, Note S5 and Figure S1). The large discrepancy of $K_{d,det}$ from true K_d at high L_0/K_d (Figure 3B, Figure S1) indicates that non-additive P must not be used to calculate R in K_d determination since the true value of L_0/K_d is unknown *a priori*. If P is the default output of a commercial instrument,^{24, 25} it must be converted to r with interconversion formula (eq 23) before calculating R and conducting the standard downstream procedures of K_d determination, such as building binding isotherm and nonlinear regression.

3.1.1.3. Diffusivity-Based Methods

A signal from the ligand (used in eq 7) must change upon complex formation. The target-ligand complex is larger than

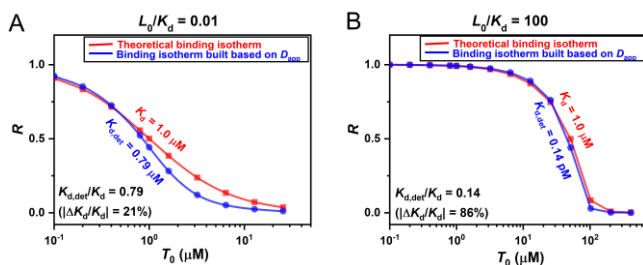


Figure 4. Comparison of the results produced by using apparent diffusion coefficient as signal (blue) and theoretical results (red) for $L_0/K_d = 0.01$ (A) and $L_0/K_d = 100$ (B).

unbound ligand and this size difference creates a foundation for size-dependent signals. A larger size results in slower translational movement leading to velocity as a signal (as discussed in section 3.1.1.1 above). A larger size leads to slower rotational depolarization resulting in anisotropy as a signal (as discussed in section 3.1.1.2 above). Furthermore, a larger size leads to slower diffusion and, accordingly, the apparent diffusion coefficient D_{app} of the ligand was suggested and used as a signal in K_d determination. One of the methods utilizing D_{app} is based on monitoring Taylor dispersion of the ligand molecule in a laminar pipe flow within a capillary filled with the target.⁴³⁻⁴⁵ No inherent sources of inaccuracy have been reported for this approach so far. Here, we decided to analyze D_{app} for additivity, required for its use as signal in eq 7 for calculation of R .

Two geometrically different implementations of finding K_d via determination of the apparent diffusion coefficient (via monitoring Taylor dispersion) have been suggested:⁴³⁻⁴⁵ one method utilizes a short plug of the equilibrium mixture of T and L, the other uses a continuous flow of the equilibrium mixture. In each method, the apparent diffusion coefficient, D_{app} , is found by fitting the signal proportional to the corresponding function with D_{app} as an unknown parameter.^{44, 46} In this work, we will not compare these two implementations of determining D_{app} , but only analyze if D_{app} is additive.

There are four components in the equilibrium mixture: L (unbound ligand), T (unbound target), C (target–ligand complex), and one solvent. If D_{app} is additive, it must satisfy:

$$D_{app} = D_{app,L} \frac{L}{L_0} + D_{app,C} \frac{C}{L_0} \quad (25)$$

where $D_{app,L}$ and $D_{app,C}$ are the apparent diffusion coefficients for pure ligand L and pure complex C, respectively, and D_{app} is the apparent diffusion coefficient of L (resulting from both the unbound and target-bound ligand) in the equilibrium mixture. The analysis of diffusion in a multi-component system requires the extended Fick's first law.^{47, 48} The quaternary system of L, T, C, and a solvent involves a diffusion coefficient matrix of 9 diffusion coefficients.⁴⁸ To simplify the system, here we assume that T and C are indistinguishable in their diffusion coefficients (i.e., the size of the target molecule is much larger than that of the ligand, and, accordingly, T and C have similar sizes), then the system is reduced to a ternary system (two components: L and T or C in one solvent). If we can prove the non-additivity of D_{app} in this simplified system, we can conclude D_{app} is a non-additive signal in general cases. In this simplified system, since we are only interested in the detectable L either in a free form or in the complex, we are considering only L and C for the diffusion matrix:

$$\hat{D} = \begin{bmatrix} D_L & D_{L,C} \\ D_{C,L} & D_C \end{bmatrix} \quad (26)$$

where D_L and D_C are the self-diffusion coefficients of L and C, respectively. $D_{C,L}$ and $D_{L,C}$ are the cross-diffusion coefficients describing the coupling between the diffusion flux of L and C. An extension of the solution proposed by Taylor was devised for a

ternary system. The normalised Taylor dispersion signal $S(t)$ of a ternary system (with respect to time t) is given by:⁴⁹

$$S(t) = (t_R / t)^{1/2} \left[\frac{B_1}{B_1 + B_2} \exp\left(-\frac{12D_{app,L}(t-t_R)^2}{r^2 t}\right) + \frac{B_2}{B_1 + B_2} \exp\left(-\frac{12D_{app,C}(t-t_R)^2}{r^2 t}\right) \right] \quad (27)$$

where

$$B_1 = \left[\begin{array}{l} (D_C - D_{C,L})R \\ + (D_L - D_{L,C})(1-R) - D_{app,L} \end{array} \right] D_{app,L}^{1/2}$$

$$B_2 = - \left[\begin{array}{l} (D_L - D_{L,C})(1-R) \\ + (D_C - D_{C,L})R - D_{app,C} \end{array} \right] D_{app,C}^{1/2}$$

Here r is the radius of the capillary and t_R is the residence time of the detected peaks of ligand. It is worth noting that the (apparent) self-diffusion coefficients $D_{app,L}$ and $D_{app,C}$ in eq 25 correspond to their binary diffusion coefficients in the limit where the concentration of their partner component, i.e. C and L respectively, goes to zero.⁵⁰ In general, cross-diffusion coefficients are functions of both the type and concentration of species and have a significant impact on the resulting apparent diffusion coefficients.^{51, 52} However, the cross-diffusion coefficients can be neglected in very dilute solutions, i.e. solutions where the molar fraction of the solvent is much greater than the molar fractions of L and C.⁴⁹ In K_d determination for tightly bound complexes, the concentration of solvent is usually in the millimolar range compared to that of ligand and complex which are at most in the picomolar to micromolar range. In this case, the molar fraction of the solvent is at least three orders of magnitude greater than the molar fractions of L and C, which allows us to simulate the Taylor dispersion signals $S(t)$ using eq 27 with neglecting the unknown cross-diffusion coefficients, i.e., $D_{C,L}$ and $D_{L,C}$.

To investigate if the apparent diffusion coefficient is an additive signal for determining accurate K_d , we simulated signals $S(t)$ using eq 27 and determined $K_{d,det}$ by assuming D_{app} satisfies eq 25 (see details in Note S6). As shown in the results of simulations in Figure 4, employing the additivity assumption of eq 25 results in large systematic errors, especially for high L_0/K_d (Figure 4B). Consequently, we consider the diffusion coefficient, along with Taylor-dispersion methods, unsuitable for accurately determining K_d .

Although the apparent diffusion coefficient cannot be directly used to calculate R due to its non-additivity, R can be determined by analyzing an additive signal (e.g., fluorescence) that varies with the fraction of unbound ligand due to the differing diffusivities of L and C.¹⁷ Species with different diffusion coefficients can undergo incomplete separation in laminar flow, a phenomenon known as TIS (transient incomplete separation).⁵³⁻⁵⁵ Based on the theory of TIS, we developed the method of “accurate constant via transient incomplete separation” (ACTIS) using laser-induced fluorescence (LIF) or mass spectroscopy (MS) as the detection method.¹⁷ ACTIS has been validated to be accurate, robust, and rugged both in computer simulations and with physical instruments.⁵⁶⁻⁵⁸

3.1.2. Mis-calibration of Signal-detecting Instrument and Inaccurate Calibration Parameters

K_d determination relies on measuring signal changes due to complex formation. For accurate R values, the instrument detecting the ligand must be properly calibrated, ensuring a linear relationship between the detected signal and concentration. Mis-calibrated instruments can introduce systematic errors in R , affecting the accuracy of $K_{d,det}$. The necessity of appropriate calibration for signal-detecting instruments is well-known, and the calibration procedures vary from instrument to instrument.⁵⁹⁻⁶¹ In

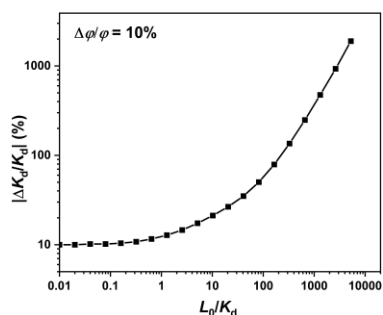


Figure 5. The dependence of relative systematic error of $K_{d,det}$ (i.e., $|\Delta K_d/K_d|$) on L_0/K_d with adding 10% relative systematic error in φ (i.e., $\Delta\varphi/\varphi = 10\%$) for a complete-separation approach with fluorescence as the signal.

Supporting Information (Note S7 and Figure S2), we demonstrate the effect of a mis-calibrated fluorescence detector on $K_{d,det}$.

Calibration parameters are often used in data analysis to standardize detected signals.^{16, 40, 62} Accurate calibration parameters need to be determined prior to K_d -determination experiments. Errors in calibration parameters lead to errors in calculated R , impacting the accuracy of $K_{d,det}$. As an example, we study the effects of errors in two calibration parameters — φ (quantum yield of target-bound ligand relative to that of unbound ligand in fluorescence detection) and G (grating factor in fluorescence anisotropy) — on the accuracies of $K_{d,det}$. Additionally, we discuss methods to enhance the accuracy of these calibration parameters.

3.1.2.1. Quantum Yield in Fluorescence Detection

In K_d -determination approaches detecting changes in fluorescence intensity due to the target's binding to the ligand (where the ligand denotes the component labelled with a fluorophore and of smaller size), fluorescence quenching (i.e., quantum yield change of a fluorophore) often occurs when the ligand binds to the target.⁶³ In complete-separation approaches, such as nonequilibrium capillary electrophoresis of equilibrium mixtures (NECEEM), R is calculated with eq 5 which involves a calibration parameter, φ — the quantum yield of the target-bound ligand relative to that of the unbound ligand.^{16, 28, 29} Here, we compare $K_{d,det}$ to true K_d by introducing a 10% relative systematic error to φ (i.e., $\Delta\varphi/\varphi = 0.1$) across a wide range of L_0/K_d (Figure 5). The large relative systematic error in $K_{d,det}$ ($|\Delta K_d/K_d|$) at high L_0/K_d (as depicted in Figure 5) underscores the importance of accurately determining φ in complete-separation approaches.

In complete-separation approaches, φ is determined by comparing the signal area under the peak for pure complex (S_C^*) to the area for pure ligand (S_L^*):^{16, 28, 29}

$$\varphi = \frac{S_C^*}{S_L^*} \quad (28)$$

Determining accurate φ necessitates finding S_L^* and S_C^* from pure ligand and pure complex, respectively, with identical concentrations, and accurately measuring the corresponding areas. To meet these requirements, we first need to decide on what concentration of ligand L_0 to use in order to produce S_L^* in eq 28. While using the ligand concentration of $L_0 = \text{LOQ}$ minimizes systematic errors in $K_{d,det}$ derived from systematic errors in L_0 , T_0 , and R ,²⁰ we recommend employing a higher ligand concentration of $L_0 \geq 10 \times \text{LOQ}$ in the preliminary experiment to determine S_L^* . A sample with higher ligand concentration (e.g., $L_0 = 10 \times \text{LOQ}$) can yield a larger and more easily defined area of S_L^* (and S_C^*), leading to more accurate measured signal areas and reducing errors in determined φ .

To measure the area of S_C^* from pure complex with the same concentration, i.e., L_0 , the conditions outlined in eq 8 must be met to bind all ligands with a total concentration of L_0 . To increase the likelihood of meeting the condition of $T_0 \gg K_d$ (unknown) (eq 8),

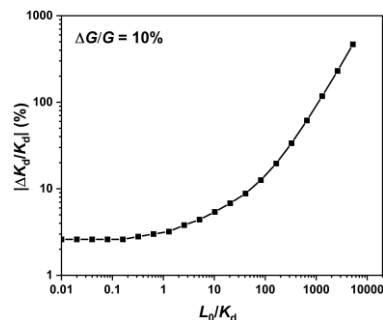


Figure 6. The dependence of relative systematic error of $K_{d,det}$ (i.e., $|\Delta K_d/K_d|$) on L_0/K_d with adding 10% relative systematic error in G factor (i.e., $\Delta G/G = 10\%$) for anisotropy-based K_d determination.

the equilibrium mixture used for measuring S_C^* , should contain the highest possible target concentration T_0 , which is the solubility of the target in the sample buffer. Note that the increase in sample viscosity caused by high T_0 would unlikely affect the accuracy of measured S_C^* in complete-separation approaches because signals (peak areas) are independent of viscosities. Furthermore, to ensure the condition of $T_0 > L_0$ (in eq 8) is met, L_0 used in determining S_L^* and S_C^* cannot be excessively high. Therefore, we recommend using $L_0 = 10 \times \text{LOQ}$ and $T_0 = \text{“solubility of target”}$ as the component concentrations in the equilibrium mixture for measuring S_C^* . It is important to emphasize that all conditions of preliminary experiments, e.g., temperature, sample buffer, detection system, etc., must be identical to those in the subsequent K_d -determination experiments to ensure the determined φ is a correct calibration parameter in downstream data analysis.

Unlike complete-separation approaches, incomplete-separation approaches, e.g., ACTIS, do not require the parameter φ to correct signal S_C^* in eq 7 for calculating R , since the detected fluorescence intensity multiplied with a constant quenching coefficient satisfies the requirement of signal superposition (eq 6).¹⁷ Thus, although fluorescence quenching affects the detected signal S , its presence does not affect the accuracy of $K_{d,det}$ obtained in the approaches with incomplete separation of free ligand from complex.

3.1.2.2. Grating Factor in Fluorescence Anisotropy

Experimentally, the fluorescence anisotropy (r) of a fluorophore is determined with:^{40, 64, 65}

$$r = \frac{I_{VV} - GI_{VH}}{I_{VV} + 2GI_{VH}} \quad (29)$$

where I_{VV} and I_{VH} are the detected emission intensities with vertical and horizontal polarizations, respectively, when the excitation light is vertically polarized. G is a grating factor used to correct the instrumental bias on vertically and horizontally polarized lights, which can be determined by:^{40, 64, 65}

$$G = \frac{I_{HV}}{I_{HH}} \quad (30)$$

where I_{HV} and I_{HH} are the emission intensities with vertical and horizontal polarizations, respectively, when the excitation light is horizontally polarized. Any systematic error in G will lead to inaccurate r , and consequently translate into systematic errors in R and $K_{d,det}$. To study the effect of inaccurate G on the accuracy of $K_{d,det}$, we demonstrate the dependence of systematic error in $K_{d,det}$ on L_0/K_d with adding an experimentally reasonable 10% relative systematic error in G (i.e., $\Delta G/G = 0.1$) (Figure 6). Figure 6 shows that the effect of the inaccuracy of G on the accuracy of $K_{d,det}$ is severe at high L_0/K_d , e.g., at $L_0/K_d = 10^3$ and 10% systematic error in G , the relative systematic error in $K_{d,det}$ is greater than 100%. Since true K_d is unknown *a priori* in a K_d -determination experiment, L_0/K_d may be large even when using the lowest suitable L_0 for quantification, i.e., $L_0 = \text{LOQ}$. Thus, determining an accurate

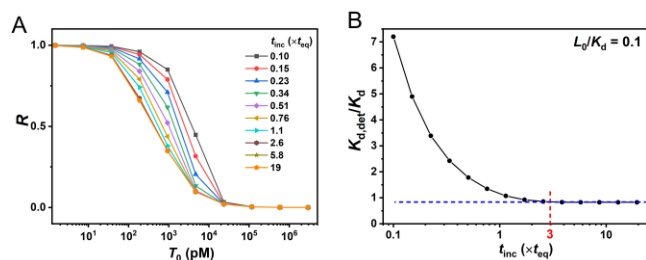


Figure 7. The dependencies of representative binding isotherms (A) and $K_{d,det}/K_d$ (B) on incubation time t_{inc} . In the simulations, L_0/K_d was chosen to be 0.1. Due to the assumption of pseudo-first order conditions (either $T_0 \ll L_0$ and $L \approx L_0$ or $L_0 \ll T_0$ and $T \approx T_0$) satisfied by each EM, the stabilized $K_{d,det}$ was slightly smaller than the input K_d , i.e., stabilized $K_{d,det}/K_d$ was slightly smaller than unit, which does not affect estimating the sufficient incubation time.

G factor is crucial for determining accurate K_d with fluorescence anisotropy.

To measure the grating factor G , as suggested by eq 30, the excitation light must be horizontally polarized. Horizontally polarized excitation light ensures that the fluorophores' excited-state distribution is along the detection axis, thereby equalizing the intensities of emitted light with different polarization orientations on the plane of detection, which is perpendicular to the travel direction of the emitted light.^{59, 60} In this scenario, any difference in the detected intensities of vertically and horizontally polarized emissions is caused by instrumental bias, which can be corrected by the determined G factor. Since G is dependent on wavelength and instrumental setup,^{34, 59} its value should be re-determined when any optical component, e.g., emission filter and excitation/emission polarizer, is changed in the instrument.

3.1.3. Not Reaching Equilibrium or Saturation

Careful and correct pre-experimental calculations and experimental design are crucial for the accurate determination of K_d . In these preparative steps, researchers should decide on: (i) the most suitable K_d -determination approach for the studied binding pair, (ii) experimental conditions, such as temperature and wavelength of the light source, (iii) the concentration of each binding partner in each equilibrium mixture, (iv) incubation time for the samples, etc. Among these experimental parameters, the total concentrations of binding partners in equilibrium mixtures (i.e., L_0 and T_0) and the incubation time for the samples are usually difficult to choose due to the lack of reliable input information. Here we demonstrate the effect of insufficient incubation time and failure to reach saturation in the binding isotherm (caused by mis-selection of concentrations) on the accuracy of $K_{d,det}$. We provide suggestions on how to ensure the incubation time is sufficient and how to ensure that the equilibrium mixture with the highest T_0 satisfies the saturation condition.

3.1.3.1. Not Reaching Equilibrium in Binding Reaction

The first experimental step of the classic methodology of K_d determination is to prepare a set of equilibrium mixtures containing a constant concentration of the limiting component L_0 and varied concentrations T_0 of the target. To minimize the systematic error in $K_{d,det}$ propagated from ΔL_0 , ΔT_0 , and ΔR , we should choose $L_0 = LOQ$.²⁰ In practice, the lowest nonzero T_0 is usually chosen as low as possible (often much lower than L_0),⁶⁶ for which the pseudo-first order conditions of $T_0 \ll L_0$ and $L \approx L_0$ are satisfied. Therefore, the characteristic time t_{eq} (eq 16) of the reversible binding reaction (eq 1) with the lowest nonzero T_0 is expressed as:

$$t_{eq} \approx (k_{off} + k_{on} L_0)^{-1} \quad (31)$$

$$\text{or } t_{eq} \approx (k_{off} + k_{on} LOQ)^{-1} \text{ when } L_0 = LOQ$$

which limits (represents the longest) characteristic time for all the binding reactions with different T_0 in a single K_d -determination

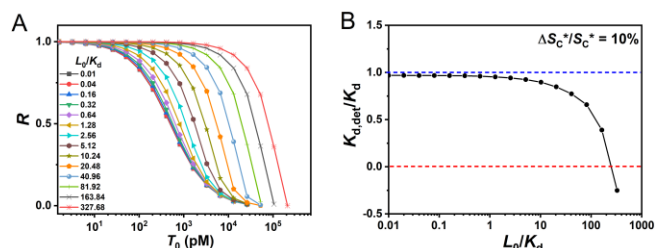


Figure 8. The dependencies of representative binding isotherms (A) and $K_{d,det}/K_d$ (B) on L_0/K_d with adding 10% relative systematic error in S_C^* , i.e., the measured S_C^* is 10% higher than true S_C^* determined at saturation. In these simulations, we assume the cumulative signal S decreases with the increase of T_0 .

experiment. To reach $\geq 95\%$ of the equilibrium concentration of the complex with the lowest nonzero T_0 , the incubation time (t_{inc}) must reach at least 3 times of the t_{eq} shown in eq 31 (Note S8). In the studies of molecular pairs with high affinity (i.e., low K_d with high k_{on} and/or low k_{off}) and using low L_0 in all samples, the sufficient incubation time (i.e., $t_{inc} \geq 3t_{eq}$) can be extremely long (e.g., a few days) (Note S8). Thus, it is common to overestimate K_d due to using insufficient incubation time.⁶⁷

To demonstrate the effect of insufficient incubation time on the accuracy of $K_{d,det}$, we simulated the binding isotherms using the spreadsheet Data S1. We utilized the incubation time within a range of $0.1t_{eq}$ to $19t_{eq}$ (t_{eq} was calculated using eq 31) with a 1.5-fold step size with $L_0/K_d = 0.1$ (Figure 7A) and summarized the dependence of $K_{d,det}/K_d$ on the incubation time (Figure 7B). The results of simulations (Figure 7B) show that, even with low $L_0/K_d = 0.1$, insufficient incubation time can cause $K_{d,det}$ to be folds higher than the true K_d . Both the binding isotherm and $K_{d,det}$ stabilize when $t_{inc} \geq 3t_{eq}$ as expected. Although there are some experimental and mathematical approaches to estimate sufficient incubation time (Note S9), at this stage, the only reliable method of eliminating the effect of incubation time on the accuracy of $K_{d,det}$ is conducting multiple K_d -determination experiments with increased incubation times until $K_{d,det}$ stabilizes.⁶⁷ Note that, as equilibration time is longer at lower T_0 , one can plan a sequence of experiments so that equilibrium mixtures with higher T_0 are analyzed before equilibrium mixtures with lower T_0 allowing the latter more time for equilibration.

3.1.3.2. Not Reaching Saturation in Binding Isotherm

For K_d -determination approaches with complete separation of unbound ligand from target-bound ligand, although a complete binding isotherm with R ranging from 0 to 1 is preferable, a partial binding isotherm can be used to determine K_d if the quantum yield ratio ϕ is accurately predetermined (eq 28). However, in most K_d -determination approaches, free ligand and complex cannot be completely separated, and R is calculated with eq 7, in which the signals from pure ligand and pure complex (i.e., S_L^* and S_C^*) play crucial roles. As we mentioned above, the measurement of S_L^* is trivial, while the determination of S_C^* requires that the binding reaction reach saturation condition, i.e., $C \gg L$. Since all the R values are calculated based on S_L^* and S_C^* (eq 7), an inaccurate S_C^* , i.e., a binding isotherm does not reach saturation, can distort the whole binding isotherm and reduce the accuracy of $K_{d,det}$ to a large degree.

Here, we simulated binding isotherms (with Data S1) by adding 10% relative systematic error in S_C^* (i.e., binding isotherm does not reach saturation and $\Delta S_C^*/S_C^* = 0.1$) for a large range of L_0/K_d (Figure 8A), and summarized the dependence of $K_{d,det}/K_d$ ratio on L_0/K_d (Figure 8B). Figure 8B indicates that, for binding isotherms not reaching saturation conditions, $K_{d,det}$ can be much lower than the true K_d (even reach the impossible negative values) at high L_0/K_d , emphasizing the importance of using T_0 that allows the binding isotherm to reach saturation condition.

To ensure that the binding isotherm reaches saturation, the

conditions of the equilibrium mixture with the highest T_0 should satisfy eq 8, i.e., $T_0 > L_0$ and $T_0 \gg K_d$. The condition of $T_0 > L_0$ is easy to satisfy if L_0 is chosen to be close to LOQ of the instrument (usually in pico- to nano-molar range), while it is difficult to conclude if the condition of $T_0 \gg K_d$ is satisfied without knowing the true K_d . A potential solution to this problem is to use the largest possible target concentration T_0 (which represents the solubility of the target in the sample buffer), in the equilibrium mixture (as discussed in section 3.1.2.1 for determining ϕ in complete-separation approaches). However, this solution has two main limitations for incomplete-separation approaches. First, using excessively high T_0 itself may affect the accuracy of measured Sc^* . For instance, the increased viscosity of the sample caused by high T_0 (e.g., protein concentration) can affect the detected signals for diffusivity-based (or -related) approaches such as ACTIS and MST. Second, if the binding isotherm reaches saturation with T_0 which is much smaller than solubility, reaching the highest possible T_0 would waste a large amount of the target, which is often a precious protein. Therefore, to ensure that a binding isotherm reaches saturation and to avoid the drawbacks associated with using excessively high T_0 , we suggest a criterion for the saturation in a binding isotherm. The criterion entails ensuring that zero lies within the uncertainty range of the slope for the linear fitting of “cumulative signal S versus T_0 ” obtained from the equilibrium mixtures with the three highest T_0 . Additionally, the highest T_0 should be at least twofold greater than the lowest T_0 in the three equilibrium mixtures.

3.1.4. Estimating Systematic Error in R Quantitatively

To provide researchers a comprehensive guidance to minimize the systematic error in R , we summarize the measures discussed above into a checklist which is an expanded version of the checklist proposed by Jarmoskaite *et al.* (see Table S1).⁶⁷ By using the checklist of Table S1, researchers can reduce the likelihood of common theoretical or experimental mistakes in determining R and thus significantly reduce ΔR . Based on the experimentalist’s confidence in the determined calibration parameters and the accuracy of the instruments used to measure signals, etc., the range of minimized $\Delta R/R$ (relative systematic error of R) with a certain confidence level might be estimated. However, at this stage, we have not identified an approach for quantitatively determining the interval of minimized systematic error of R that can be used as a reliable input to calculate the systematic error range of $K_{d,det}$. Note that, the random error of R (δR) is independent to ΔR and is translated into the random error of $K_{d,det}$ (σ) through nonlinear regression of a binding isotherm.

3.2. Sources of Systematic Errors in Concentrations

Sources of systematic errors in T_0 and L_0 arise from various factors. If concentrations are calculated based on the weight of solid material and volume of solvent, imperfectly calibrated mass- and volume-measuring equipment as well as errors in product purity can lead to systematic errors in concentrations. If concentrations are calculated using spectrophotometry (Lambert-Beer law), systematic errors in molar extinction coefficients will result in systematic errors in concentrations. These common sources can induce systematic errors in target and ligand concentrations of stock solutions, which, in turn, can propagate into systematic errors in concentrations of other diluted solutions used in K_d -determination experiments. Another common source of systematic errors in T_0 and L_0 occurring at any step of an experiment is solute adsorption onto pipette tips, vials, channels, etc. Here, we illustrate the effect of systematic errors in T_0 and L_0 on the accuracy of $K_{d,det}$ for a large range of L_0/K_d (Figure 9), and delve into the common sources of systematic errors in concentrations along with strategies to mitigate them. Additionally, we introduce an approach of estimating confidence intervals of minimized systematic errors in T_0 and L_0 , which can be potentially used to assess the accuracy of

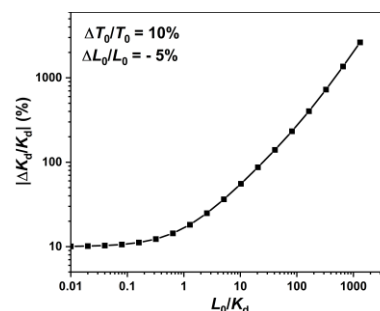


Figure 9. The dependence of relative systematic error of $K_{d,det}$ (i.e., $|\Delta K_d/K_d|$) on L_0/K_d with adding 10% relative systematic error in T_0 and -5% relative systematic error in L_0 , i.e., the nominal T_0 is 10% higher than true T_0 and the nominal L_0 is 5% lower than true L_0 .

$K_{d,det}$ in future works.

3.2.1. Mis-calibration and Improper Operation of Measuring Equipment

K_d determination using the nonlinear regression approach entails preparing a series of equilibrium mixtures with constant L_0 and varied T_0 . Experimentally, all the equilibrium mixtures are prepared from the high-concentration stock solutions of ligand and target.⁶⁸⁻⁷⁰ Thus, any systematic errors in concentrations of stock solutions will translate to systematic errors in L_0 and T_0 for all equilibrium mixtures. In certain experiments, a stock solution is created by dissolving a specific weight of solid material into a volume of solvent (e.g., buffer) to achieve a desired concentration. In such cases, the mis-calibration or improper operation of mass- and volume-measuring equipment can introduce systematic errors in the concentration of a stock solution.

Mass-measuring equipment in a chemistry laboratory typically includes lab balances, such as top-loading balances and analytical balances.⁷¹ All types of lab balances must be correctly and regularly calibrated to minimize systematic errors in measured masses. Traditionally, lab balances are manually calibrated to adjust the balance reading using standard weights.⁷² Many modern lab balances feature automatic self-calibration functions, simplifying and expediting the calibration process. Combining manual and automatic calibrations ensures the best accuracy of a calibrated balance.⁷²⁻⁷⁴ Alongside proper calibration, users must adhere to common guidelines to achieve high accuracy and precision in mass measurements, including levelling the balance horizontally, maintaining cleanliness, and taring the balance before measurements.⁷⁴ Detailed instructions on correctly calibrating and operating lab balances are provided in the Supporting Information (Note S10).

A wide array of specialized volume-measuring equipment is usually available in well-equipped laboratories, including beakers, flasks, graduated cylinders, burettes, and pipettes.⁷⁵ Since most studied binding partners are valuable materials (e.g., proteins), well-established K_d -determination approaches typically require small quantities.⁷⁶⁻⁷⁹ Therefore, using volume pipettes alone is often sufficient for volume measurements in a K_d -determination experiment. To ensure high accuracy and precision in measured volumes, volume pipettes must be routinely calibrated and operated correctly. Pipettes should be calibrated every 3–6 months, and after thorough cleaning.⁸⁰ Calibration involves establishing the relationship between the volume and mass of distilled water aspirated/dispensed by the pipette.⁸⁰ Following calibration, proper pipetting techniques, such as pre-wetting the pipette tip before aspirating liquids and touching off after each dispense, should be followed to enhance accuracy.⁸¹ Detailed guidelines on correctly calibrating and operating pipettes are provided in the Supporting Information (Note S11).

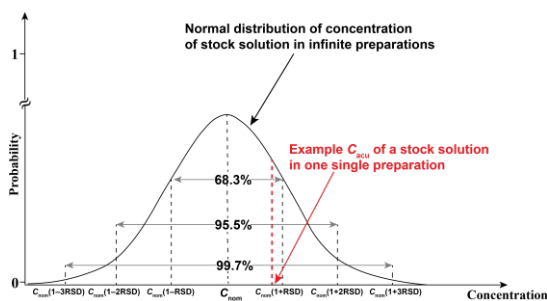


Figure 10. Demonstration of the relationship between the accurate concentration (C_{acu}) of a stock solution in one single preparation and the concentration distribution in an infinite number of preparations. With minimized systematic error in concentration, we assume the average concentration is equal to the nominal concentration C_{nom} .

3.2.2. Product impurity

The purified material of binding partners (target and ligand) is either obtained from commercial vendors or produced internally in a laboratory. The quality and purity of the purified material vary from batch to batch.⁸² Since any impurity or degradation of binding partners will result in systematic errors in concentrations, preventing reagent degradation and determining their purity are crucial for reducing systematic errors in L_0 and T_0 . In Supporting Information (Note S12), we discuss how to avoid reagent degradation using ssDNA and protein as exemplified ligand and target, respectively.

To minimize systematic errors in concentrations, researchers often employ spectrophotometry (Lambert-Beer law) to measure “true” concentrations. However, this method has two limitations: (i) spectrophotometry cannot distinguish impurities or contaminations from the product, and (ii) systematic errors in molar extinction coefficients will translate into systematic errors in concentrations. Thus, if the purities of ligand and target products are unknown *a priori*, they must be determined using analytical approaches. For example, high-performance liquid chromatography (HPLC) and CE can quantitatively determine the purity of ssDNA,^{83, 84} and sodium dodecyl sulfate–polyacrylamide gel electrophoresis (SDS-PAGE) and liquid chromatography–mass spectrometry (LC-MS) can estimate the purity of proteins.^{85, 86} Based on the quantitatively determined purities of products, the concentrations calculated from measured mass and volume or determined by spectrophotometry need to be corrected.

On the other hand, determining the accurate concentration of a pure product in solution using the Lambert-Beer law requires knowledge of the accurate molar extinction coefficient for the component in solution, which is influenced by various chemical conditions such as buffer type, ionic strength, and pH.⁸⁷ Hence, when using a widely accepted molar extinction coefficient to calculate the concentration of a component, one should ensure that the conditions of the measured solution are similar (if not exactly the same) to conditions used to determine the molar extinction coefficient. Otherwise, the concentration determined with the Lambert-Beer law according to a known molar extinction coefficient should be considered inaccurate.⁸⁷ In many cases, accurate molar extinction coefficients for studied components are unavailable; thus, the systematic errors in L_0 and T_0 can only be reduced by correcting the concentrations based on the experimentally determined purities of the reagents.

3.2.3. Solute adsorption

Systematic errors in concentrations can also result from solute adsorption, i.e., reagent adsorption, which occurs in most steps of a K_d -determination experiment. Reagent adsorption can significantly reduce reagent concentration at low concentrations, which is typically the case for $L_0 = LOQ$ and T_0 in a low-concentration range.⁸⁸ Solute adsorption to pipette tips and sample vials can occur during sample preparation, while solute adsorption

to fluidic paths and channels may occur during sample analysis.^{89, 90} Although reagent adsorption cannot be fully eliminated, it can be minimized by careful experimental design and optimization.

Common measures of reducing reagent adsorption include adding blocking agents in solutions, modifying surfaces with biocompatible coatings, and using experimental parts/equipment made of low-binding materials. These approaches are discussed in detail in the Supporting Information (Note S13).⁹¹⁻⁹³

3.2.4. Confidence Interval of Systematic Errors in Concentrations

To assist researchers in minimizing systematic error in concentrations L_0 and T_0 , the measures discussed above are summarized in Table S1 in the Supporting Information. Estimating the systematic error in $K_{d,det}$ — using the logic described in Figure 1B — requires input values for ΔL_0 , ΔT_0 , and ΔR . If exact values of systematic errors in variables are known, then the case is trivial as the variable can be simply corrected for this systematic error. Conversely, if nothing is known about systematic errors in variables, then the problem is ill-posed as completely unknown systematic errors cannot be propagated. However, there is a third case where the exact values of systematic errors in variables are unknown, but the confidence intervals of the systematic errors with desired confidence levels can be quantitatively assessed. Confidence intervals of systematic errors are not commonly discussed in statistics, they likely play a crucial role in the determination of physicochemical parameters with nonlinear regression. Here, we discuss two cases of assessing confidence intervals of systematic errors in concentrations.

The first case involves a rough estimation based on experiences, akin to the estimation of $\Delta R/R$ range mentioned in section 3.1.4. If techniques listed in section 3.2.2 (e.g., SDS-PAGE) for determining large systematic errors or approaches of method optimization (e.g., surface-modification) are inaccessible, an experienced experimentalist should be able to estimate the maximum ranges of relative systematic errors in concentrations with some confidence, e.g., $\pm 20\%$ for ligand concentration and $\pm 30\%$ for target concentration with confidence.

The second case involves a quantitative assessment based on the relative random errors (i.e., relative standard deviations, RSD) in concentrations of stock solutions. If all necessary procedures for minimizing systematic errors (e.g., device calibration, purity measurement, and method optimization) have been properly conducted, we can reasonably assume that the systematic errors in L_0 and T_0 of equilibrium mixtures are from the random errors in the concentrations of ligand and target stock solutions, i.e., the normally distributed concentrations of stock solutions in infinite preparations (Figure 10). This assumption is valid because all the diluted solutions used in K_d determination with nonlinear regression are prepared from one single condensed ligand stock solution and one single condensed target stock solution, and the random errors in concentrations of stock solutions (exist in infinite number of sample preparations) are usually much greater than that of equilibrium mixtures due to its more complicated preparation procedure with more error sources. Thus, the confidence intervals of systematic errors in L_0 and T_0 (in equilibrium mixtures) can be estimated by measuring the RSD of the concentrations of their stock solutions in multiple preparations. Since there is no reliable measure to determine concentration directly, RSD of concentrations should be determined by experimentally measuring the spectroscopic signals (e.g., light absorption or fluorescence intensity) from stock solutions in multiple preparations (see an example in Table S2).

For a single preparation of stock solution with a nominal (desired) concentration C_{nom} , the confidence interval (e.g., with 68.3% confidence level) of systematic error can be calculated as $\Delta C \in [-C_{nom} \times RSD, C_{nom} \times RSD]$, for which the confidence interval of accurate concentration C_{acu} is $C_{acu} \in [C_{nom}(1 - RSD), C_{nom}(1 + RSD)]$ (Figure 10). Note that, the confidence level of

systematic error or accurate concentration can be varied by using different numbers of RSD in the calculation of confidence intervals. As a result, due to equilibrium mixtures being prepared from diluted stock solutions, the confidence intervals (e.g., with 68.3% confidence level) of systematic errors in nominal L_0 and T_0 can be assessed as $\Delta L_0 \in [-\text{RSD} \times L_0, \text{RSD} \times L_0]$ and $\Delta T_0 \in [-\text{RSD} \times T_0, \text{RSD} \times T_0]$, respectively. It is important to emphasize that the confidence interval of ΔL_0 and ΔT_0 derived from the RSD of concentrations of stock solutions are the lower limit of systematic error ranges assuming that all other systematic errors in the concentrations of stock solutions have been eliminated. Despite lacking an approach for quantitatively assessing the confidence interval of ΔR , the lower limits of confidence intervals of ΔL_0 and ΔT_0 explained here can be potentially used to assess the lower limit of confidence interval of ΔK_d with error propagation.

4. Concluding Remarks

Since the systematic error in a determined K_d ($\Delta K_{d,\text{det}}$) is translated from the systematic errors in the variables used to determine K_d , i.e., ΔL_0 , ΔT_0 , and ΔR (Figure 1B), understanding the sources of systematic errors in all variables and minimizing these errors are pivotal to minimizing $\Delta K_{d,\text{det}}$. To determine an accurate K_d , the first step (often ignored by researchers) is to ensure there is no theoretical or experimental mistake in the K_d -determination approach. Such mistakes can introduce systematic errors in R , and eventually translate into systematic error in $K_{d,\text{det}}$, which can be extremely large at unfavorable (large) values of L_0/K_d (see, for example, Figure 2). In this work, we discussed the most common sources of systematic errors in R , such as non-additive signals, mis-calibrated instruments, inaccurate calibration parameters, ect., and quantitatively studied the effect of errors from these sources on the accuracy of $K_{d,\text{det}}$. We also provided suggestions on how to reduce or eliminate the systematic error in R caused by the common error sources. With careful theoretical and experimental design and proper instrument calibration, ΔR can be minimized, while the confidence interval of the minimized ΔR cannot be quantitatively determined.

The sources of systematic errors in concentrations (i.e., ΔL_0 , ΔT_0), such as mis-calibrated measuring equipment, product impurities, and reagent adsorption, have been well-studied and many approaches to eliminate these error sources have been developed.^{80, 83, 85, 91} In this work, we reiterated the importance of minimizing ΔL_0 and ΔT_0 by demonstrating the effect of experimentally reasonable systematic errors in concentrations on the accuracy of $K_{d,\text{det}}$ (Figure 9). We discussed the approaches for eliminating the common sources for ΔL_0 and ΔT_0 , such as careful equipment calibration, avoiding reagent degradation, and minimizing solute adsorption. We summarized the measures of eliminating or minimizing ΔR , ΔL_0 and ΔT_0 caused by the common error sources into a checklist (Table S1), which is a convenient tool for researchers in the field of K_d determination. For a specific K_d -determination approach, researchers should establish a standard operating procedure (SOP) for minimizing systematic errors in concentrations based on the chemical properties of the ligand and target used. The SOP should be established prior to any experiment, and it should be strictly followed during the K_d -determination experiments.

Although the systematic errors in concentrations cannot be fully eliminated, and their true values can hardly be determined accurately, the confidence intervals of the minimized systematic errors in concentrations can be quantitatively assessed with the quantitative study of random errors in concentrations of stock solutions. We foresee that, by combining the quantitatively assessed confidence intervals of systematic errors in concentrations and numerical error propagation for nonlinear regression (not discussed in this work), the lower limit of confidence interval of systematic error in $K_{d,\text{det}}$ can be determined.

ASSOCIATED CONTENT

Supporting Information

The Supporting Information is available free of charge at <https://XXX>

Definition of signal additivity and the calculation of the fraction of unbound ligand R with additive signals (Note S1); Proof of additivity of signals that linearly depend on concentrations (Note S2); Sensitivity of determined K_d to random errors in variables for R approaching either zero or unity (Note S3); Non-additivity of polarization (Note S4); The dependence of relative systematic error of $K_{d,\text{det}}$ on L_0/K_d for using non-additive polarization to calculate R (Note S5, Figure S1); Non-additivity of diffusion coefficients (Note S6, Figure S2); Demonstration of the effect of mis-calibrated instrument on the accuracy of $K_{d,\text{det}}$ (Note S7, Figure S3); Sufficiency of incubation time (Note S8); Experimental and mathematical approaches to estimate sufficient incubation time (Note S9); Calibration and operations of lab balances (Note S10); Calibration and operations of pipettes (Note S11); Avoiding reagent degradation (Note S12); Common measures for reducing solute adsorption (Note S13); Checklist for minimizing the systematic errors of variables in K_d determination with nonlinear regression (Table S1); Determination of the random error in the concentration of fluorescein (ligand) solutions (Table S2).

AUTHOR INFORMATION

Corresponding Author

Sergey N. Krylov – Department of Chemistry and Centre for Research on Biomolecular Interactions, York University, Toronto, Ontario M3J 1P3, Canada; orcid.org/0000-0003-3270-2130; Email: skrylov@yorku.ca

Authors

Tong Ye Wang – Department of Chemistry and Centre for Research on Biomolecular Interactions, York University, Toronto, Ontario M3J 1P3, Canada; orcid.org/0000-0001-9462-7194

Jean-Luc Rukundo – Department of Chemistry and Centre for Research on Biomolecular Interactions, York University, Toronto, Ontario M3J 1P3, Canada; orcid.org/0000-0003-3626-2515

Zhiyuan Mao – Department of Chemistry and Centre for Research on Biomolecular Interactions, York University, Toronto, Ontario M3J 1P3, Canada; orcid.org/0009-0008-2578-5525

Notes

The authors declare no competing financial interest.

ACKNOWLEDGMENTS

This work was supported by funds from York University towards the Catalyzing Interdisciplinary Research Cluster “Technologies for Identification and Control of Infectious Diseases”.

REFERENCES

- (1) Kenakin, T.; Williams, M. Defining and characterizing drug/compound function. *Biochemical pharmacology* **2014**, *87* (1), 40-63.
- (2) Petrauskas, V.; Kazlauskas, E.; Gedgaudas, M.; Baranauskienė, L.; Zubrienė, A.; Matulis, D. Thermal shift assay for protein–ligand dissociation constant determination. *TrAC Trends in Analytical Chemistry* **2023**, 117417.
- (3) Dahl, G.; Akerud, T. Pharmacokinetics and the drug–target residence time concept. *Drug Discovery Today* **2013**, *18* (15-16), 697-707.

- (4) Chock, P. B.; Rhee, S. G.; Stadtman, E. R. Interconvertible enzyme cascades in cellular regulation. *Annual Review of Biochemistry* **1980**, *49* (1), 813-841.
- (5) Miles, L.; Plow, E. Plasminogen receptors: ubiquitous sites for cellular regulation of fibrinolysis. *Fibrinolysis* **1988**, *2* (2), 61-71.
- (6) Bottari, F.; Daems, E.; de Vries, A.-M.; Van Wielendaele, P.; Trashin, S.; Blust, R.; Sobott, F.; Madder, A.; Martins, J. C.; De Wael, K. Do aptamers always bind? The need for a multifaceted analytical approach when demonstrating binding affinity between aptamer and low molecular weight compounds. *Journal of the American Chemical Society* **2020**, *142* (46), 19622-19630.
- (7) Fielding, L. NMR methods for the determination of protein-ligand dissociation constants. *Progress in Nuclear Magnetic Resonance Spectroscopy* **2007**, *51* (4), 219-242.
- (8) Hoare, S. R.; Fleck, B. A.; Williams, J. P.; Grigoriadis, D. E. The importance of target binding kinetics for measuring target binding affinity in drug discovery: a case study from a CRF1 receptor antagonist program. *Drug Discovery Today* **2020**, *25* (1), 7-14.
- (9) Archakov, A. I.; Govorun, V. M.; Dubanov, A. V.; Ivanov, Y. D.; Veselovsky, A. V.; Lewi, P.; Janssen, P. Protein-protein interactions as a target for drugs in proteomics. *Proteomics* **2003**, *3* (4), 380-391.
- (10) Strange, P. G. Antipsychotic drugs: importance of dopamine receptors for mechanisms of therapeutic actions and side effects. *Pharmacological reviews* **2001**, *53* (1), 119-134.
- (11) Tracy, T. S.; Hummel, M. A. Modeling kinetic data from in vitro drug metabolism enzyme experiments. *Drug metabolism reviews* **2004**, *36* (2), 231-242.
- (12) Halford, S. E. An end to 40 years of mistakes in DNA-protein association kinetics? *Biochemical Society Transactions* **2009**, *37* (2), 343-348.
- (13) Sims, R. J.; Reinberg, D. Histone H3 Lys 4 methylation: caught in a bind? *Genes & development* **2006**, *20* (20), 2779-2786.
- (14) Fielding, L. NMR methods for the determination of protein-ligand dissociation constants. *Current topics in medicinal chemistry* **2003**, *3* (1), 39-53.
- (15) Jerabek-Willemsen, M.; Wienken, C. J.; Braun, D.; Baaske, P.; Duhr, S. Molecular interaction studies using microscale thermophoresis. *Assay and drug development technologies* **2011**, *9* (4), 342-353.
- (16) Kanoatov, M.; Galievsky, V. A.; Krylova, S. M.; Cherney, L. T.; Jankowski, H. K.; Krylov, S. N. Using nonequilibrium capillary electrophoresis of equilibrium mixtures (NECEEM) for simultaneous determination of concentration and equilibrium constant. *Analytical chemistry* **2015**, *87* (5), 3099-3106.
- (17) Sisavath, N.; Rukundo, J. L.; Le Blanc, J. Y.; Galievsky, V. A.; Bao, J.; Kochmann, S.; Stasheuski, A. S.; Krylov, S. N. Transient incomplete separation facilitates finding accurate equilibrium dissociation constant of protein-small molecule complex. *Angewandte Chemie* **2019**, *131* (20), 6707-6711.
- (18) Rusling, J. F. Computerized method for mechanistic classification of one-electron potentiostatic current-potential curves. *Analytical Chemistry* **1983**, *55* (11), 1713-1718.
- (19) Johnson, M. L.; Correia, J. J.; Yphantis, D. A.; HalvorSON, H. R. Analysis of data from the analytical ultracentrifuge by nonlinear least-squares techniques. *Biophysical journal* **1981**, *36* (3), 575-588.
- (20) Wang, T. Y.; Ji, H.; Everton, D.; Le, A. T.; Krylova, S. M.; Fournier, R.; Krylov, S. N. Fundamental Determinants of the Accuracy of Equilibrium Constants for Affinity Complexes. *Analytical Chemistry* **2023**, *95* (42), 15826-15832.
- (21) Weber, G. Polarization of the fluorescence of macromolecules. I. Theory and experimental method. *Biochem J* **1952**, *51* (2), 145-155. DOI: 10.1042/bj0510145 From NLM.
- (22) Gradinaru, C. C.; Marushchak, D. O.; Samim, M.; Krull, U. J. Fluorescence anisotropy: from single molecules to live cells. *Analyst* **2010**, *135* (3), 452-459.
- (23) Park, S.-H.; Raines, R. T. Fluorescence polarization assay to quantify protein-protein interactions. *Protein-Protein Interactions: Methods and Applications* **2004**, 161-165.
- (24) Nosjean, O.; Souchaud, S.; Deniau, C.; Geneste, O.; Cauquil, N.; Boutin, J. A. A simple theoretical model for fluorescence polarization binding assay development. *SLAS Discovery* **2006**, *11* (8), 949-958.
- (25) Yan, K.; Hunt, E.; Berge, J.; May, E.; Copeland, R. A.; Gontarek, R. R. Fluorescence polarization method to characterize macrolide-ribosome interactions. *Antimicrobial agents and chemotherapy* **2005**, *49* (8), 3367-3372.
- (26) *Omega Series Operating Manual*. BMG LABTECH, 2017. <https://med-fom-avgaylab.sites.olt.ubc.ca/files/2018/04/0415B0001K-Operating-Manual-Omega.pdf> (accessed 2024 03-09).
- (27) *Synergy HI Operator's Manual*. BioTek® Instruments, Inc., 2012. <https://www.lebonheur.org/research/investigator-resources/manuals/BioTek%20Synergy%20HI%20Hybrid%20M-ulti-Mode%20Plate%20Reader%20manual.pdf> (accessed 2024 03-09).
- (28) Teclemichael, E.; Le, A. T.; Krylova, S. M.; Wang, T. Y.; Krylov, S. N. Bulk Affinity Assays in Aptamer Selection: Challenges, Theory, and Workflow. *Analytical Chemistry* **2022**, *94* (44), 15183-15188.
- (29) Le, A. T.; Krylova, S. M.; Krylov, S. N. Determination of the Equilibrium Constant and Rate Constant of Protein-Oligonucleotide Complex Dissociation under the Conditions of Ideal-Filter Capillary Electrophoresis. *Analytical chemistry* **2019**, *91* (13), 8532-8539.
- (30) Williamson, M. P. Using chemical shift perturbation to characterise ligand binding. *Progress in nuclear magnetic resonance spectroscopy* **2013**, *73*, 1-16.
- (31) Piñeiro, L.; Novo, M.; Al-Soufi, W. Fluorescence emission of pyrene in surfactant solutions. *Advances in colloid and interface science* **2015**, *215*, 1-12.
- (32) Zhao, Q.; Tao, J.; Feng, W.; Uppal, J. S.; Peng, H.; Le, X. C. Aptamer binding assays and molecular interaction studies using fluorescence anisotropy-a review. *Analytica chimica acta* **2020**, *1125*, 267-278.
- (33) Krylova, S. M.; Dove, P. M.; Kanoatov, M.; Krylov, S. N. Slow-dissociation and slow-recombination assumptions in nonequilibrium capillary electrophoresis of equilibrium mixtures. *Analytical chemistry* **2011**, *83* (19), 7582-7585.
- (34) Jusko, W. J.; Molins, E. A.; Ayyar, V. S. Seeking nonspecific binding: assessing the reliability of tissue dilutions for calculating fraction unbound. *Drug Metabolism and Disposition* **2020**, *48* (10), 894-902.
- (35) Dubský, P.; Dvořák, M.; Ansorge, M. Affinity capillary electrophoresis: the theory of electromigration. *Analytical and bioanalytical chemistry* **2016**, *408*, 8623-8641.
- (36) Okhonin, V.; Berezovski, M. V.; Krylov, S. N. MASKE: Macroscopic approach to studying kinetics at equilibrium. *Journal of the American Chemical Society* **2010**, *132* (20), 7062-7068.
- (37) Krylov, S. N. Kinetic CE: foundation for homogeneous kinetic affinity methods. *Electrophoresis* **2007**, *28* (1 - 2), 69-88.
- (38) Tanaka, Y.; Terabe, S. Estimation of binding constants by capillary electrophoresis. *Journal of Chromatography B* **2002**, *768* (1), 81-92.
- (39) Wang, Y.; Adeoye, D. I.; Ogunkunle, E. O.; Wei, I.-A.; Filla, R. T.; Roper, M. G. Affinity capillary electrophoresis: a critical review of the literature from 2018 to 2020. *Analytical Chemistry* **2020**, *93* (1), 295-310.
- (40) Jameson, D. M.; Ross, J. A. Fluorescence polarization/anisotropy in diagnostics and imaging. *Chemical reviews* **2010**, *110* (5), 2685-2708.
- (41) Wolff, M. Polarization of light reflected from rough planetary surface. *Applied Optics* **1975**, *14* (6), 1395-1405.
- (42) Jablonski, A. On the notion of emission anisotropy. *Bull. Acad. Pol. Sci* **1960**, *8*, 259-264.

- (43) Clark, S. M.; Konermann, L. Determination of ligand–protein dissociation constants by electrospray mass spectrometry-based diffusion measurements. *Analytical chemistry* **2004**, *76* (23), 7077-7083.
- (44) Jensen, H.; Østergaard, J. Flow induced dispersion analysis quantifies noncovalent interactions in nanoliter samples. *Journal of the American Chemical Society* **2010**, *132* (12), 4070-4071.
- (45) Bielejewska, A.; Bylina, A.; Duszczyc, K.; Fiałkowski, M.; Holyst, R. Evaluation of ligand-selector interaction from effective diffusion coefficient. *Analytical chemistry* **2010**, *82* (13), 5463-5469.
- (46) Clark, S. M.; Leaist, D. G.; Konermann, L. Taylor dispersion monitored by electrospray mass spectrometry: a novel approach for studying diffusion in solution. *Rapid communications in mass spectrometry* **2002**, *16* (15), 1454-1462.
- (47) Annunziata, O.; Buzatu, D.; Albright, J. G. Protein diffusion coefficients determined by macroscopic-gradient Rayleigh interferometry and dynamic light scattering. *Langmuir* **2005**, *21* (26), 12085-12089.
- (48) Guevara-Carrion, G.; Gaponenko, Y.; Janzen, T.; Vrabc, J.; Shevtsova, V. Diffusion in multicomponent liquids: From microscopic to macroscopic scales. *The Journal of Physical Chemistry B* **2016**, *120* (47), 12193-12210.
- (49) Leaist, D. G. Ternary diffusion coefficients of 18-crown-6 ether–KCl–water by direct least-squares analysis of Taylor dispersion measurements. *Journal of the Chemical Society, Faraday Transactions* **1991**, *87* (4), 597-601.
- (50) Cussler, E. L. *Diffusion: mass transfer in fluid systems*; Cambridge university press, 2009.
- (51) Price, W. E. Theory of the Taylor dispersion technique for three-component-system diffusion measurements. *Journal of the Chemical Society, Faraday Transactions 1: Physical Chemistry in Condensed Phases* **1988**, *84* (7), 2431-2439.
- (52) Callendar, R.; Leaist, D. G. Diffusion coefficients for binary, ternary, and polydisperse solutions from peak-width analysis of Taylor dispersion profiles. *Journal of solution chemistry* **2006**, *35*, 353-379.
- (53) Griffiths, A. On the movement of a coloured index along a capillary tube, and its application to the measurement of the circulation of water in a closed circuit. *Proceedings of the Physical Society of London* **1910**, *23* (1), 190.
- (54) Taylor, G. I. Dispersion of soluble matter in solvent flowing slowly through a tube. *Proceedings of the Royal Society of London. Series A. Mathematical and Physical Sciences* **1953**, *219* (1137), 186-203.
- (55) Trumbore, C. N.; Grehlinger, M.; Stowe, M.; Keleher, F. M. Further experiments on a new, fast method for determining molecular weights of diffusing species in a liquid phase. *Journal of Chromatography A* **1985**, *322*, 443-454.
- (56) Wang, T. Y.; Rukundo, J.-L.; Le, A. T.; Ivanov, N. A.; Le Blanc, J. Y.; Gorin, B. I.; Krylov, S. N. Transient Incomplete Separation of Species with Close Diffusivity to Study the Stability of Affinity Complexes. *Analytical Chemistry* **2022**, *94* (44), 15415-15422.
- (57) Rukundo, J.-L.; Kochmann, S.; Wang, T. Y.; Ivanov, N. A.; Le Blanc, J. Y.; Gorin, B. I.; Krylov, S. N. Template Instrumentation for “Accurate Constant via Transient Incomplete Separation”. *Analytical Chemistry* **2021**, *93* (34), 11654-11659.
- (58) Rukundo, J.-L.; Le Blanc, J. Y.; Kochmann, S.; Krylov, S. N. Assessing Accuracy of an Analytical Method in silico: Application to “Accurate Constant via Transient Incomplete Separation”(ACTIS). *Analytical Chemistry* **2020**, *92* (17), 11973-11980.
- (59) Schulte, J.; Tants, J.-N.; von Ehr, J.; Schlundt, A.; Morgner, N. Determination of dissociation constants via quantitative mass spectrometry. *Frontiers in Analytical Science* **2023**, *3*, 1119489.
- (60) Kempen, E. C.; Brodbelt, J. S. A method for the determination of binding constants by electrospray ionization mass spectrometry. *Analytical chemistry* **2000**, *72* (21), 5411-5416.
- (61) Rincken, T.; Rincken, A.; Tenno, T.; Järv, J. Calibration of glucose biosensors by using pre-steady state kinetic data. *Biosensors and Bioelectronics* **1998**, *13* (7-8), 801-807.
- (62) Canbay, H. S. Spectrophotometric determination of acid dissociation constants of some arylpropionic acids and arylacetic acids in acetonitrile-water binary mixtures at 25°C. *Brazilian Journal of Pharmaceutical Sciences* **2023**, *58*, e20740.
- (63) Van de Weert, M.; Stella, L. Fluorescence quenching and ligand binding: A critical discussion of a popular methodology. *Journal of Molecular Structure* **2011**, *998* (1-3), 144-150.
- (64) Lakowicz, J. R.; Lakowicz, J. R. Fluorescence anisotropy. *Principles of fluorescence spectroscopy* **1999**, 291-319.
- (65) Rendon, D. A.; Palacio, J. L. A modern, simple, and economical accessory for continuous L-format measurement of steady-state fluorescence anisotropy. *Analytical Biochemistry* **2022**, *639*, 114473.
- (66) Hulme, E. C.; Trevethick, M. A. Ligand binding assays at equilibrium: validation and interpretation. *British journal of pharmacology* **2010**, *161* (6), 1219-1237.
- (67) Jarmoskaite, I.; AlSadhan, I.; Vaidyanathan, P. P.; Herschlag, D. How to measure and evaluate binding affinities. *Elife* **2020**, *9*, e57264.
- (68) DeBlasi, A.; O'Reilly, K.; Motulsky, H. J. Calculating receptor number from binding experiments using same compound as radioligand and competitor. *Trends in pharmacological sciences* **1989**, *10* (6), 227-229.
- (69) Huang, R.; Leung, I. K. Protein–small molecule interactions by WaterLOGSY. *Methods in enzymology* **2019**, *615*, 477-500.
- (70) Dalvit, C.; Hadden, D. T.; Sarver, R. W.; Ho, A. M.; Stockman, B. J. Multi-selective one dimensional proton NMR experiments for rapid screening and binding affinity measurements. *Combinatorial chemistry & high throughput screening* **2003**, *6* (5), 445-453.
- (71) *How Laboratory Scales Work & How Leasing Benefits Labs.* excedr, 2024. <https://www.excedr.com/general-lab-equipment/lab-balance> (accessed 2024 03-18).
- (72) O'Driscoll, A. *A Guide to Balance and Scale Calibration.* Laboratory Supply Network, Inc., 2018. <https://labbalances.net/blogs/blog/balance-and-scale-calibration-guide> (accessed 2024 03-20).
- (73) *Analytical Balances with Internal Calibration.* METTLER TOLEDO, 2024. [https://www.mt.com/us/en/home/products/Laboratory_Weighing_Solutions/analytical-balances/analytical-balances-with-internal-calibration.html?filter\[balance-line\]=ML-T&filter\[balance-line\]=XPR](https://www.mt.com/us/en/home/products/Laboratory_Weighing_Solutions/analytical-balances/analytical-balances-with-internal-calibration.html?filter[balance-line]=ML-T&filter[balance-line]=XPR) (accessed 2024 03-18).
- (74) French, L. *The Do's and Don'ts of Laboratory Balances.* Labcompare, 2023. <https://www.labcompare.com/10-Featured-Articles/596136-The-Do-s-and-Don-ts-of-Laboratory-Balances/> (accessed 2024 03-18).
- (75) Kumari, R.; Anand, A. *Physical Chemistry Laboratory Manual*; IK International Pvt Ltd, 2018.
- (76) Heegaard, N. H.; Nilsson, S.; Guzman, N. A. Affinity capillary electrophoresis: important application areas and some recent developments. *Journal of Chromatography B: Biomedical Sciences and Applications* **1998**, *715* (1), 29-54.
- (77) Tjernberg, A.; Carnö, S.; Oliv, F.; Benkestock, K.; Edlund, P.-O.; Griffiths, W. J.; Hallén, D. Determination of dissociation constants for protein–ligand complexes by electrospray ionization mass spectrometry. *Analytical chemistry* **2004**, *76* (15), 4325-4331.
- (78) Espina, V.; Mehta, A. I.; Winters, M. E.; Calvert, V.; Wulfkuhle, J.; Petricoin III, E. F.; Liotta, L. A. Protein microarrays: molecular profiling technologies for clinical specimens. *Proteomics* **2003**, *3* (11), 2091-2100.
- (79) Podobnik, M.; Kraševc, N.; Zavec, A. B.; Naneh, O.; Flašker, A.; Caserman, S.; Hodnik, V.; Anderluh, G. How to study protein-protein interactions. *Acta Chimica Slovenica* **2016**, *63* (3).

- (80) Saha, S. *Performing Pipette Calibration Yourself*. Bitesize Bio, 2021. <https://bitesizebio.com/40766/performing-pipette-calibration-yourself/> (accessed 2024 03-18).
- (81) *10 Steps to Improve Pipetting Accuracy*. Thermo Fisher Scientific 2024. <https://www.thermofisher.com/ca/en/home/life-science/lab-plasticware-supplies/lab-plasticware-supplies-learning-center/lab-plasticware-supplies-resource-library/fundamentals-of-pipetting/proper-pipetting-techniques/10-steps-to-improve-pipetting-accuracy.html> (accessed 2024 03-18).
- (82) Patra, A.; Herrera, M.; Gutiérrez, J. M.; Mukherjee, A. K. The application of laboratory - based analytical tools and techniques for the quality assessment and improvement of commercial antivenoms used in the treatment of snakebite envenomation. *Drug Testing and Analysis* **2021**, *13* (8), 1471-1489.
- (83) Andrus, A.; Bloch, W. HPLC of oligonucleotides and polynucleotides. *HPLC Macromol* **1998**, *872*, 141.
- (84) Smith, A.; Nelson, R. J. Capillary electrophoresis of DNA. *Current protocols in molecular biology* **2004**, *68* (1), 2.8. 1-2.8. 17.
- (85) Raynal, B.; Lenormand, P.; Baron, B.; Hoos, S.; England, P. Quality assessment and optimization of purified protein samples: why and how? *Microbial cell factories* **2014**, *13*, 1-10.
- (86) Woods, R. J.; Xie, M. H.; Von Kreudenstein, T. S.; Ng, G. Y.; Dixit, S. B. LC-MS characterization and purity assessment of a prototype bispecific antibody. In *MABs*, 2013; Taylor & Francis: Vol. 5, pp 711-722.
- (87) Lottenberg, R.; Jackson, C. M. Solution composition dependent variation in extinction coefficients for p-nitroaniline. *Biochimica et Biophysica Acta (BBA)-Protein Structure and Molecular Enzymology* **1983**, *742* (3), 558-564.
- (88) Lin, S.; Shih-Yuan Lee, A.; Lin, C.-C.; Lee, C.-K. Determination of binding constant and stoichiometry for antibody-antigen interaction with surface plasmon resonance. *Current Proteomics* **2006**, *3* (4), 271-282.
- (89) Maes, K.; Smolders, I.; Michotte, Y.; Van Eeckhaut, A. Strategies to reduce aspecific adsorption of peptides and proteins in liquid chromatography-mass spectrometry based bioanalyses: An overview. *Journal of Chromatography A* **2014**, *1358*, 1-13.
- (90) Righetti, P. G.; Sebastiano, R.; Citterio, A. Capillary electrophoresis and isoelectric focusing in peptide and protein analysis. *Proteomics* **2013**, *13* (2), 325-340.
- (91) Bange, A.; Halsall, H. B.; Heineman, W. R. Microfluidic immunosensor systems. *Biosensors and Bioelectronics* **2005**, *20* (12), 2488-2503.
- (92) Malherbe, C. J.; De Beer, D.; Joubert, E. Development of on-line high performance liquid chromatography (HPLC)-biochemical detection methods as tools in the identification of bioactives. *International journal of molecular sciences* **2012**, *13* (3), 3101-3133.
- (93) Ranade, A. V.; Mukhtarov, R.; An Liu, K. J.; Behrner, M. A.; Sun, B. Characterization of sample loss caused by competitive adsorption of proteins in vials using sodium dodecyl sulfate-polyacrylamide gel electrophoresis. *Langmuir* **2019**, *35* (12), 4224-4232.
- (94) Latham, J. C.; Stein, R. A.; Bornhop, D. J.; Mchaourab, H. S. Free-solution Label-free Detection of α -crystallin Chaperone Interactions by Back-scattering Interferometry. *Analytical chemistry* **2009**, *81* (5), 1865-1871.
- (95) Weeramange, C. J.; Fairlamb, M. S.; Singh, D.; Fenton, A. W.; Swint - Kruse, L. The strengths and limitations of using biolayer interferometry to monitor equilibrium titrations of biomolecules. *Protein Science* **2020**, *29* (4), 1004-1020.
- (96) Orosz, F.; Ovádi, J. A simple method for the determination of dissociation constants by displacement ELISA. *Journal of immunological methods* **2002**, *270* (2), 155-162.
- (97) Liao, J.-y.; Song, Y.; Liu, Y. A new trend to determine biochemical parameters by quantitative FRET assays. *Acta Pharmacologica Sinica* **2015**, *36* (12), 1408-1415.
- (98) Miyabe, K.; Ishitobi, A.; Hiyama, K.; Kubotani, F. Moment Analysis Method for Measurement of Reaction Equilibrium and Rate Constants by Using High-Performance Liquid Chromatography. *Analytical Chemistry* **2024**.
- (99) Winzor, D. J. Quantitative affinity chromatography. *Journal of Biochemical and Biophysical Methods* **2001**, *49* (1-3), 99-121.
- (100) Krainer, G.; Broecker, J.; Vargas, C.; Fanghänel, J. r.; Keller, S. Quantifying high-affinity binding of hydrophobic ligands by isothermal titration calorimetry. *Analytical chemistry* **2012**, *84* (24), 10715-10722.
- (101) Ward, W. H.; Holdgate, G. A. 7 Isothermal Titration Calorimetry in Drug Discovery. *Progress in medicinal chemistry* **2001**, *38*, 309-376.
- (102) Zhang, M. Y. Understanding cyclotricatechylene and cryptophanes ligands for forming supramolecular assemblies that selectively coordinate heavy metal cations by mass spectrometry. UNSW Sydney, 2022.
- (103) Svobodová, J.; Mathur, S.; Muck, A.; Letzel, T.; Svatoš, A. Microchip - ESI - MS determination of dissociation constant of the lysozyme-NAG3 complex. *Electrophoresis* **2010**, *31* (15), 2680-2685.
- (104) Su, X.-C.; Jergic, S.; Ozawa, K.; Burns, N. D.; Dixon, N. E.; Otting, G. Measurement of dissociation constants of high-molecular weight protein-protein complexes by transferred 15 N-relaxation. *Journal of biomolecular NMR* **2007**, *38*, 65-72.
- (105) Murthy, G.; Venkatesh, N. Determination of kinetic parameters of epitope-paratope interaction based on solid phase binding: An inexpensive alternate to biospecific interaction analysis. *Journal of Biosciences* **1996**, *21*, 641-651.
- (106) Cottet, H.; Biron, J.-P.; Martin, M. Taylor dispersion analysis of mixtures. *Analytical chemistry* **2007**, *79* (23), 9066-9073.

SUPPORTING INFORMATION

ABC of K_d Accuracy

Tong Ye Wang,^{1,2} Jean-Luc Rukundo,^{1,2} Zhiyuan Mao,^{1,2} Sergey N. Krylov*,^{1,2}

¹Department of Chemistry, York University, Toronto, Ontario M3J 1P3, Canada

²Centre for Research on Biomolecular Interactions, York University, Toronto, Ontario M3J 1P3, Canada

*Corresponding author's email: skrylov@yorku.ca

Table of Contents

Note S1: Definition of signal additivity and the calculation of the fraction of unbound ligand R with additive signals.....	S3
Note S2: Proof of additivity of signals that linearly depend on concentrations.....	S4
Note S3: Sensitivity of determined K_d to random errors in variables for R approaching either zero or unity	S4
Note S4: Non-additivity of polarization.....	S5
Note S5: The dependence of relative systematic error of $K_{d,det}$ on L_0/K_d for using non-additive polarization to calculate R (Figure S1)	S6
Note S6: Non-additivity of diffusion coefficients (Figure S2)	S7
Note S7: Demonstration of the effect of mis-calibrated instrument on the accuracy of $K_{d,det}$ (Figure S3)	S9
Note S8: Sufficiency of incubation time.....	S10
Note S9: Experimental and mathematical approaches to estimate sufficient incubation time	S11
Note S10: Calibration and operations of lab balances	S12
Note S11: Calibration and operations of pipettes	S12
Note S12: Avoiding reagent degradation.....	S13
Note S13: Common measures for reducing solute adsorption.....	S13
Table S1: Checklist for minimizing the systematic errors of variables in K_d determination with nonlinear regression	S13
Table S2: Determination of the random error in the concentration of fluorescein (ligand) solutions ..	S15
References	S16

Additional supplementary files

The following supplementary files can be found on Figshare:

DOI: 10.6084/m9.figshare.25464685

File name	Description/Experiment
Figures.zip	Figures in main text and supporting information (Origin, Adobe Illustrator, PNG, and TIFF files).
Data S1.xlsx	Spreadsheet for simulating binding isotherms (Excel file).
Checklist.pdf	Checklist for minimizing the systematic errors of variables in K_d determination with nonlinear regression (PDF file).

Note S1: Definition of signal additivity and the calculation of the fraction of unbound ligand R with additive signals

In K_d determinations, we call the measured signal (S) “additive” when it can be directly decomposed into the sum of signals contributed by the target-unbound ligand (i.e., free ligand L) and target-bound ligand (or complex C), i.e., S_L and S_C , such as:

$$S = S_L + S_C \quad (S1)$$

If Q_L and Q_C are quantities of L and C in units of quantity, e.g., moles, then,

$$S = S_{L,\text{unit}} Q_L + S_{C,\text{unit}} Q_C \quad (S2)$$

where $S_{L,\text{unit}}$ and $S_{C,\text{unit}}$ are the signals from unit quantities of unbound ligand and complex (i.e., target-bound ligand), respectively. If Q is the total quantity of L and C , such as:

$$Q = Q_L + Q_C \quad (S3)$$

then,

$$\begin{aligned} S &= (S_{L,\text{unit}} Q) \frac{Q_L}{Q} + (S_{C,\text{unit}} Q) \frac{Q_C}{Q} \\ \Rightarrow S &= S_{L,\text{per quantity } Q} \frac{Q_L}{Q} + S_{C,\text{per quantity } Q} \frac{Q_C}{Q} \\ \Rightarrow S &= S_{L,\text{per quantity } Q} f_L + S_{C,\text{per quantity } Q} f_C \end{aligned} \quad (S4)$$

where f_L and f_C are the fractions of L and C in the total quantity of them.

Let's assume the total quantity Q is a constant, S_L^* is the signal from quantity Q of L , and S_C^* is the signal from quantity Q of C , then eq S4 is converted to:

$$S = S_L^* f_L + S_C^* f_C \quad (S5)$$

If the unit of quantity is concentration, then eq S5 can be expressed as:

$$S = S_L^* \frac{L}{L+C} + S_C^* \frac{C}{L+C} \quad (S6)$$

where L and C are equilibrium concentrations of the ligand and complex, respectively. If the total concentration of ligand L_0 is a constant (i.e., $L_0 = L + C = \text{const}$), then eq S6 can be rewritten as:

$$S = S_L^* \frac{L}{L_0} + S_C^* \frac{C}{L_0} \quad (S7)$$

According to the definition of the fraction of unbound ligand R ($R = L/L_0$, eq 4 in the main text), eq S7 is rewritten as:

$$S = S_L^* R + S_C^* (1 - R) \quad (S8)$$

By solving R from eq S8, we obtain:

$$R = \frac{S - S_C^*}{S_L^* - S_C^*} \quad (S9)$$

which is eq 7 in the main text. For using eq S9 to calculate R values (for constructing binding isotherms), eq S1 must be satisfied, which is the additivity of signals. Note that, eq S5 is applicable to surface-based methods, e.g., SPR (Surface Plasmon Resonance) and BLI (Biolayer Interferometry), as well.^{1,2}

Note S2: Proof of additivity of signals that linearly depend on concentrations

Assuming the detected signal is linearly related to components concentration, (e.g. fluorescence):³

$$\begin{aligned} S_L &= \alpha L + N, & S_C &= \beta C + N \\ S_L^* &= \alpha L_0 + N, & S_C^* &= \beta C_0 + N \end{aligned} \quad (\text{S10})$$

where S_L is the signal from unbound ligand, S_C is the signal from complex (i.e., target-bound ligand), L is the concentration of unbound ligand, C is the concentration of complex, α and β are the proportionality factors for ligand and complex, respectively, and N is the background that is (assumed to be) independent of components and their concentrations and thus only one N contributes to the cumulative signal S :

$$\begin{aligned} S &= S_L + S_C = \alpha L + \beta C + N \\ &= \alpha L_0 \frac{L}{L_0} + \beta L_0 \frac{C}{L_0} + N \frac{L_0}{L_0} = \alpha L_0 \frac{L}{L_0} + \beta L_0 \frac{C}{L_0} + N \frac{L+C}{L_0} \\ &= \alpha L_0 \frac{L}{L_0} + N \frac{L}{L_0} + \beta L_0 \frac{C}{L_0} + N \frac{C}{L_0} \\ &= (\alpha L_0 + N) \frac{L}{L_0} + (\beta L_0 + N) \frac{C}{L_0} \\ &= S_L^* \frac{L}{L_0} + S_C^* \frac{C}{L_0} \end{aligned} \quad (\text{S11})$$

which is the superposition equation (eq 6 in main text) required for an additive signal. Note that, if the background noise is dependent on the concentration of any reactant, e.g. donor/acceptor concentration in FRET (Fluorescence Resonance Energy Transfer), the background noise must be subtracted to calculate S , S_L and S_C .⁴ Otherwise, the measured signal would be non-additive.

Note S3: Sensitivity of determined K_d to random errors in variables for R approaching either zero or unity

If K_d is determined with a single R value, the following formula is used:⁵

$$K_d = \frac{T_0 - L_0(1-R)}{(1/R-1)} \quad (\text{S12})$$

By applying the regular error propagation rule to eq S3, we have:

$$\begin{aligned} \delta K_d &= \sqrt{\left(\frac{\partial K_d}{\partial T_0}\right)^2 \delta T_0^2 + \left(\frac{\partial K_d}{\partial L_0}\right)^2 \delta L_0^2 + \left(\frac{\partial K_d}{\partial R}\right)^2 \delta R^2} \\ &= \frac{\sqrt{\delta T_0^2 + \delta L_0^2(1-R)^2 + \delta R^2 \left(L_0(1/R-1) + (T_0 - L_0(1-R))/R^2\right)^2}}{(1/R-1)} \\ &= \frac{\sqrt{\delta T_0^2 R^2 + \delta L_0^2 (1-R)R^2 + \delta R^2 \left(L_0(1-R) + (T_0 - L_0(1-R))/R\right)^2}}{1-R} \end{aligned} \quad (\text{S13})$$

It has been proven that, with the single-point approach, determined K_d is the most accurate for $R \approx 1/2$.⁶ Now let's investigate the sensitivity of determined K_d to random errors of R , T_0 , and L_0 when R value approaches two extrema: 0 and 1.

When R approaches 0,

$$\begin{aligned} \lim_{R \rightarrow 0} \delta K_d &= \frac{\sqrt{\delta T_0^2 0^2 + \delta L_0^2 ((1-0) \times 0)^2 + \delta R^2 (L_0(1-0) + (T_0 - L_0(1-0))/0)^2}}{1-0} \\ &= \sqrt{\delta R^2 (L_0 - \infty)^2} \\ &= \infty \end{aligned} \quad (\text{S14})$$

When R approaches 1,

$$\begin{aligned} \lim_{R \rightarrow 1} \delta K_d &= \frac{\sqrt{\delta T_0^2 1^2 + \delta L_0^2 ((1-1) \times 1)^2 + \delta R^2 (L_0(1-1) + (T_0 - L_0(1-1))/1)^2}}{1-1} \\ &= \frac{\sqrt{\delta T_0^2 + \delta R^2 T_0^2}}{0} \\ &= \infty \end{aligned} \quad (\text{S15})$$

Eqs S14 and S15 suggest that when R approaches 0 or 1, any random error of R (or T_0) can be largely magnified when propagated to the random error of the determined K_d value. If single-point K_d -determination experiments are repeated many times, the large random error of determined K_d (obtained for R being close to 0 or 1) will result in very poor precision of the determined K_d values. If the single-point K_d -determination experiment is only conducted once or repeated a few times, the large random error of the determined K_d (obtained for R being close to 0 or 1) becomes the systematic error of the determined K_d , resulting in very poor accuracy (and precision) of the determined K_d values.

Note S4: Non-additivity of polarization

Fluorescence anisotropy (r) has been proven to be an additive signal, which satisfies:⁷

$$r = r_L \frac{L}{L_0} + r_C \frac{C}{L_0} \quad (\text{S16})$$

If polarization is additive, it must satisfy:

$$P = P_L \frac{L}{L_0} + P_C \frac{C}{L_0} \quad (\text{S17})$$

where P_L and P_C are the polarizations of pure ligand and pure complex, respectively, with a concentration of L_0 . However, by replacing r in eq S16 with eq 23 in the main text, we obtain:

$$\frac{2P}{3-P} = \frac{2P_L}{3-P_L} \frac{L}{L_0} + \frac{2P_C}{3-P_C} \frac{C}{L_0} \quad (\text{S18})$$

which cannot be converted to eq S16 with any transformations. Therefore, polarization is non-additive.

Note S5: The dependence of relative systematic error of $K_{d,det}$ on L_0/K_d for using non-additive polarization to calculate R

To investigate the effect of using non-additive polarization to calculate R on the accuracy of $K_{d,det}$, we first used Data S1 to produce the theoretical binding isotherms “ R versus T_0 ” for L_0/K_d from 0.01 to 1311 with a 2-fold step size. According to the definition of R (eq 4 in main text), eq S16 is rewritten as:

$$r = r_L R + r_C (1 - R) \quad (S19)$$

By assuming r_L and r_C to be 0 and 0.4, respectively, anisotropy r corresponding to each R value was calculated. Eq 23 in the main text can be transformed to be an expression of polarization P with anisotropy r :

$$P = \frac{3r}{2 + r} \quad (S20)$$

Using eq S20, polarizations of pure ligand (P_L) and pure complex (P_C), and P corresponding to each r were computed. With P_L , P_C , and P calculated from each r , the R values (R') determined with non-additive P for different T_0 were calculated with:

$$R' = \frac{P - P_C}{P_L - P_C} \quad (S21)$$

and formed the binding isotherms “ R' versus T_0 ” for L_0/K_d from 0.01 to 1311. By fitting isotherms “ R' versus T_0 ” with eq 10 in the main text, $K_{d,det}$ obtained by using non-additive polarization to calculate R for different L_0/K_d were determined. The resulted dependence of accuracy of $K_{d,det}$ (i.e., $|\Delta K_d/K_d|$) on L_0/K_d is summarized in Figure S1.

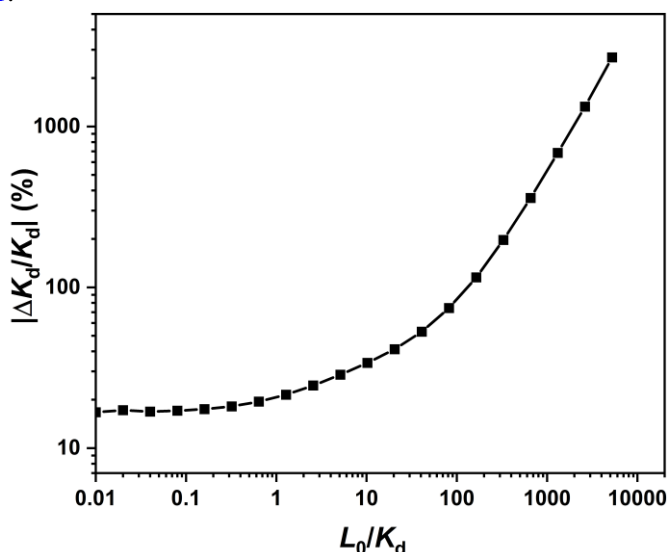


Figure S1. The dependence of relative systematic error of $K_{d,det}$ (i.e., $|\Delta K_d/K_d|$) on L_0/K_d for using non-additive polarization to calculate R .

Note S6: Non-additivity of diffusion coefficients

Determination of K_d using Taylor dispersion analysis

Taylor dispersion analysis is a method that has been widely used to characterize the diffusion coefficient of analytes in a solute within a laminar flow pipe.^{8, 9} Taylor described the concentration profile of the dispersion of an injected plug as given by:¹⁰

$$C(x, t) = y_0 + A \exp\left(-\frac{1}{2} \frac{(t - t_R)^2}{\sigma^2}\right) \quad (\text{S22})$$

where $C(x, t)$ is the signal profile averaged over the cross-section of the flow pipe at time t and distance x ; the fitting parameters y_0 , A , t_R and σ^2 are the baseline, amplitude, average elution time and temporal variance respectively.

The value of σ^2 in eq S22 is related to the apparent diffusion coefficient D_{app} of the diffusing analyte through:

$$D_{\text{app}} = r^2 t_0 / (24\sigma^2) \quad (\text{S23})$$

where r is the radius of the flow pipe.

Taylor dispersion analysis has been used to find K_d of an equilibrium mixture (EM) via the determination of the apparent diffusion coefficient D_{app} .¹⁰⁻¹² To obtain $R = L/L_0$, from which K_d can be obtained, an additivity assumption is used:

$$D_{\text{app}} = D_{\text{app,L}} \frac{L}{L_0} + D_{\text{app,C}} \frac{C}{L_0} = D_{\text{app,L}} R + D_{\text{app,C}} (1 - R) \quad (\text{S24})$$

where $D_{\text{app,L}}$ and $D_{\text{app,C}}$ are the apparent diffusion coefficients for pure ligand L and pure complex C, respectively, and D_{app} is the apparent diffusion coefficient of L (resulting from both unbound and protein-bound) in the EM.

Equilibrium Mixture (EM) ternary system

The dispersion of the EM involves 5 components: pure L, pure complex C, pure protein P and the solvent. Assuming that P and C are indistinguishable in their diffusion properties, this system can be reduced to a simpler ternary system (two components L and C in one solvent). This system is described by 4 diffusion coefficients (see eq 26 in main text): D_L and D_C which are the self-diffusion coefficients of L and C, respectively and $D_{C,L}$ and $D_{L,C}$ are the cross-diffusion coefficients describing the coupling between the diffusion flux of L and C. The apparent (*i.e.* observable) diffusion coefficients of L and C are given by the eigenvalues of the diffusion matrix (eq 26 in main text) as:^{13, 14}

$$D_{\text{app,L}} = \frac{D_L + D_C + \sqrt{(D_L - D_C)^2 + 4D_{L,C}D_{C,L}}}{2}$$
$$D_{\text{app,C}} = \frac{D_L + D_C - \sqrt{(D_L - D_C)^2 + 4D_{L,C}D_{C,L}}}{2} \quad (\text{S25})$$

It is worth noting that the (apparent) self-diffusion coefficients $D_{\text{app,L}}$ and $D_{\text{app,C}}$ in eq S24 correspond to their binary diffusion coefficients D_L and D_C in the limit where the concentration of their partner component, *i.e.* C and L respectively, goes to zero.¹⁵ In general, cross-diffusion coefficients are functions of both the type and concentration of species and may have an impact on the resulting apparent diffusion coefficients.^{16, 17} However, the cross-diffusion coefficients can be neglected in very dilute solutions, *i.e.*

solutions where the molar fraction of the solvent is much greater than the molar fractions of L and C.¹⁵ The above considerations result in:

$$\begin{aligned} D_{\text{app,L}} &= D_L \\ D_{\text{app,C}} &= D_C \approx D_P \end{aligned} \quad (\text{S26})$$

To describe the ternary system, an extension of the original Taylor dispersion expression for binary systems (eq S22) was formulated as mentioned in the main text. The adapted concentration profile $S(t)$ of such system, taking into consideration of eq S26 becomes (eq 27 in main text):¹⁸

$$S(t) = (t_R / t)^{1/2} \left[\begin{aligned} &\frac{B_1}{B_1 + B_2} \exp\left(-\frac{12D_{\text{app,L}}(t - t_R)^2}{r^2 t}\right) \\ &+ \frac{B_2}{B_1 + B_2} \exp\left(-\frac{12D_{\text{app,C}}(t - t_R)^2}{r^2 t}\right) \end{aligned} \right]$$

where

$$\begin{aligned} B_1 &= \left[\begin{aligned} &(D_C - D_{\text{C,L}})R \\ &+ (D_L - D_{\text{L,C}})(1 - R) - D_{\text{app,L}} \end{aligned} \right] D_{\text{app,L}}^{1/2} \\ B_2 &= - \left[\begin{aligned} &(D_L - D_{\text{L,C}})(1 - R) \\ &+ (D_C - D_{\text{C,L}})R - D_{\text{app,C}} \end{aligned} \right] D_{\text{app,C}}^{1/2} \end{aligned} \quad (\text{S27})$$

Simulation parameters

The simulation parameters used in eq S27 were: $t_R = 150$ s and $r = 25$ μm , which are typical scales used in Taylor dispersion analysis to satisfy conditions under which Taylor solution is valid.⁹ D_L and D_C were chosen to be 425 $\mu\text{m}^2/\text{s}$ and 50 $\mu\text{m}^2/\text{s}$, respectively, which are in the range of typical values for diffusion coefficients of L and P.^{12, 19}

To simulate titration curves, R values obtained from the theoretical dependence of R on L_0 , T_0 and K_d , were used in eq S27. The expression for R is given by:

$$R = -\frac{K_d + T_0 - L_0}{2L_0} + \sqrt{\left(\frac{K_d + T_0 - L_0}{2L_0}\right)^2 + \frac{K_d}{L_0}} \quad (\text{S28})$$

Binding isotherms from simulated signals

The simulations were performed for $K_d = 1$ μM and $L_0 = 0.01$ and 100 μM . First, the signals $S(t)$ for different R values were simulated with Data S1. Then, the simulated signals were fitted with eq S22 to find σ^2 . With the determined σ^2 , the apparent diffusion coefficients D_{app} corresponding to different T_0 were calculated with eq S23. Subsequently, the apparent R values (R_{app}) were calculated with eq S24 according to three types of signals: *i*) the signal of EM with pure L to find $D_{\text{app,L}}$ (e.g., Figure S2A); *ii*) the signal of EM with pure C to find $D_{\text{app,C}}$ (e.g., Figure S2B), and *iii*) the signal of EM with a mixture of L and C to find D_{app} (e.g., Figure S2C). By fitting the binding isotherms “ R_{app} versus T_0 ”, the K_d values ($K_{d,\text{det}}$) determined with the assumption of additivity of D_{app} were found. The comparisons of the reresulting binding isotherm

“ R_{app} versus T_0 ” (along with $K_{d,det}$) to the theoretical binding isotherms “ R versus T_0 ” (along with input K_d) for $L_0 = 0.01$ and $100 \mu\text{M}$ are shown in Figure 4 in the main text.

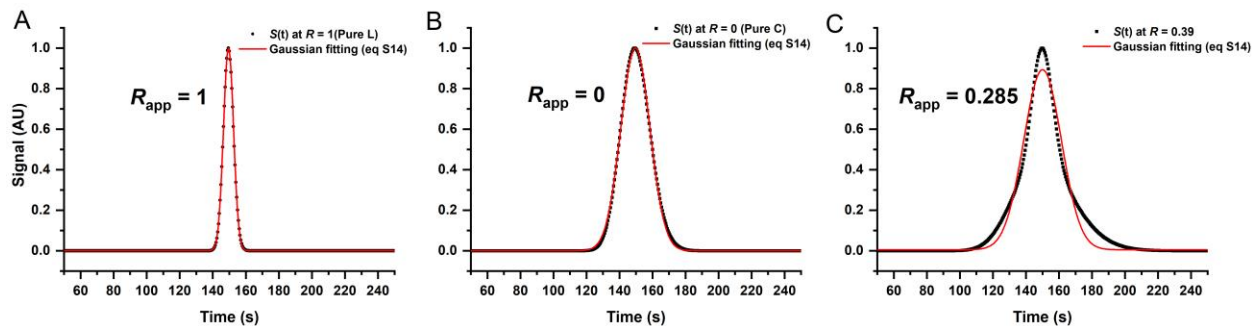


Figure S2. Examples of finding apparent diffusion coefficients along with apparent R values by fitting the simulated diffusion signals obtained with the analytical solution of Taylor dispersion. In these three examples, the input $K_d = 1 \mu\text{M}$ and $L_0 = 0.01 \mu\text{M}$.

Note S7: Demonstration of the effect of mis-calibrated instrument on the accuracy of $K_{d,det}$

In this demonstration, we use fluorescence detection as an example. As we showed in Note S1, for fluorescence signal to be additive, it should be linearly related to the concentration of fluorophore, i.e., the calibration curve of “fluorescence versus fluorophore concentration” should be linear. Otherwise, the detected signal can be non-additive. Here, we assume the dependence of fluorescence on fluorophore concentration is nonlinear, such as:

$$S = \lambda \left(\frac{C_{\text{fluor}}}{C_{\text{fluor}} + 50 \text{ pM}} \right) + 3 \quad (\text{S29})$$

where S is the detected fluorescence signal with unit of RFU (Relative Fluorescence Unit), C_{fluor} is the concentration of fluorophore with unit of pM, λ is a magnification factor (with unit of RFU) that depends on the quantum yield of the fluorophore at different binding states. The constant “3” is the magnitude of background noise with unit of RFU.

Here, we set $\lambda = 100$ RFU for unbound ligand, and $\lambda = 50$ RFU for bound ligand caused by fluorescence quenching. The resulted (nonlinear) calibration curve (A) and the discrepancies of binding isotherms and determined K_d values (at $L_0/K_d = 0.1$) caused by the instrumental nonlinear response to fluorophore concentrations (B) are demonstrated here. In the simulation, the input/true K_d was 500 pM .

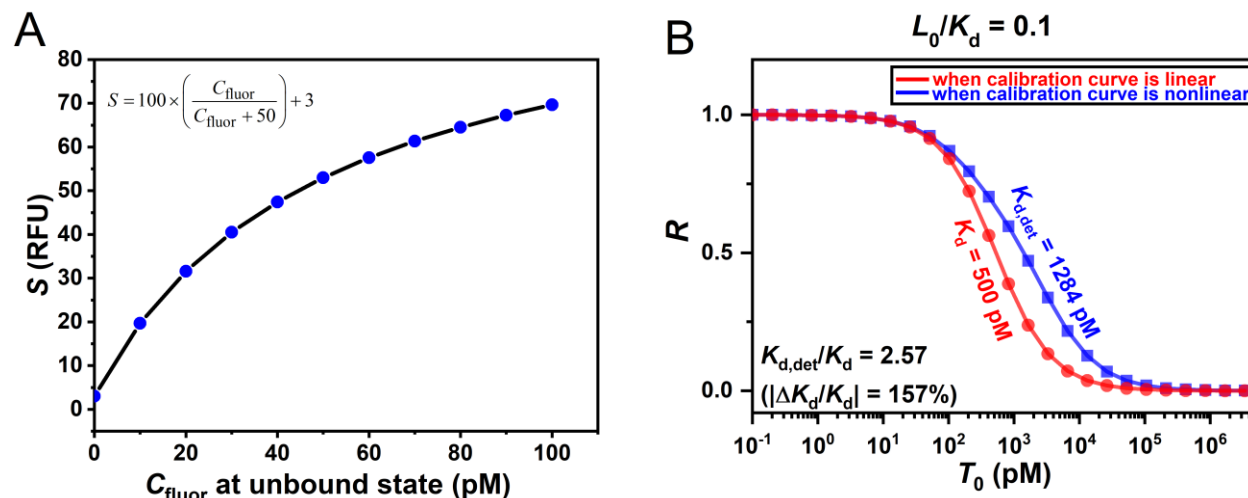


Figure S3. Demonstration of the effect of mis-calibrated instrument on the accuracy of $K_{d,det}$: **A)** An exemplified nonlinear calibration curve produced by eq S29 with setting $\lambda = 100$ RFU and 50 RFU for unbound and bound ligand, respectively; **B)** the discrepancies of binding isotherms and determined K_d values (at $L_0/K_d = 0.1$) caused by the exemplified instrumental nonlinear response to fluorophore concentrations. In the simulation, the input/true K_d was 500 pM.

Note S8: Sufficiency of incubation time

For the lowest non-zero T_0 , the pseudo-first order conditions of $T_0 \ll L_0$ and $L \approx L_0$ are satisfied. Thus, the exponential function of the dependence of the concentration of the formed complex ($C(t)$) on time (t) can be expressed as:

$$C(t) = C_{eq} \left(1 - e^{-t/t_{eq}}\right) \quad (S30)$$

with C_{eq} as the concentration of complex at equilibrium (i.e., at $t = \infty$). By replacing T_0 with L_0 , the classic characteristic equilibration time (t_{eq}) is converted to:²⁰

$$t_{eq} = (k_{on}L_0 + k_{off})^{-1} \quad (S31)$$

To reach $C(t) \geq 95\% C_{eq}$, we have:

$$\begin{aligned} C_{eq} \left(1 - e^{-t_{inc}/t_{eq}}\right) &\geq 0.95 C_{eq} \\ 1 - e^{-t_{inc}/t_{eq}} &\geq 0.95 \Rightarrow e^{-t_{inc}/t_{eq}} \leq 0.05 \\ -\frac{t_{inc}}{t_{eq}} &\leq \ln(0.05) \Rightarrow t_{inc} \geq -\ln(0.05)t_{eq} \\ t_{inc} &\geq 3t_{eq} \end{aligned} \quad (S32)$$

Therefore, the incubation time t_{inc} should be equal or longer than three times of characteristic equilibration time t_{eq} to reach $\geq 95\%$ equilibration. For example, in a K_d -determination experiment, the K_d of the studied

binding pair is 10^{-10} M with a k_{on} of $10^5 \text{ M}^{-1}\text{s}^{-1}$, and the experimentally used (constant) total concentration of ligand $L_0 = 10^{-11}$ M which is the LOQ of the instrument for detection. With eq 2 in main text, k_{off} can be calculated as 10^{-5} s^{-1} . Then, with the definition of t_{eq} in eq S31 (eq 31 in main text), t_{eq} is calculated as 9.1×10^4 s, which is ~ 25 h. As a result, the sufficient incubation time is $t_{\text{inc}} \geq 75$ h ($3t_{\text{eq}}$), which is more than 3 days.

Note S9: Experimental and mathematical approaches to estimate sufficient incubation time

The sufficient incubation time can be determined experimentally. Some kinetic methods, e.g., stopped-flow spectroscopy, can monitor a binding reaction in real-time, and intuitively show if the reaction reaches equilibrium.²¹ If a real-time reaction monitoring method capable of detecting the signal from the target (with low LOQ) is available in the lab, researchers can employ it to conduct a preliminary study for determining the incubation time with a mixture of ligand with concentration L_0 and target with concentration T_0 ($\ll L_0$) as a sample. Here, L_0 and T_0 are the constant ligand concentration and lowest nonzero target concentration planned for the K_{d} -determination experiment. Since the target is the limiting component with a smaller concentration in this preliminary study, only the signal from the target should be measured, and sufficient incubation time can be assumed to be the time for the reaction to reach 95% completion.

If a real-time reaction monitoring method is unavailable in the lab, researchers can measure the mixture of ligand with concentration L_0 and detectable target (with the lowest nonzero T_0) with a certain frequency and construct a curve for the dependence of the target's signal on time to determine the time after which the signal stops changing significantly, using this time as the incubation time. However, if there is no means of solely measuring the signal from the target or the lowest nonzero T_0 is smaller than the instrument's LOQ for the target, researchers should conduct multiple K_{d} -determination experiments with different incubation times. When $K_{\text{d,det}}$ stops decreasing with the increase of incubation time, it can be concluded that the incubation time is sufficient for all samples to reach equilibrium.²²

All experimental methods mentioned above for determining the sufficient incubation time require specialized equipment and expertise and are generally resource-intensive. Alternatively, a simple mathematical estimation with the help of eq S31 can serve the purpose of finding sufficient incubation time well in many cases. For example, when planning to study a molecular pair with an expected K_{d} value in the nanomolar range (i.e., 1 – 1000 nM) using an instrument with LOQ = 0.1 nM for the ligand, the ligand concentration L_0 is chosen to be the LOQ (0.1 nM) to minimize the error of $K_{\text{d,det}}$ translated from the errors of variables. To assess the sufficient incubation time, k_{on} can be assumed to be near an “average” value of $\sim 10^6 \text{ M}^{-1}\text{s}^{-1}$ since generally k_{on} ranges from 10^3 to $10^9 \text{ M}^{-1}\text{s}^{-1}$.²³ Then, by assuming the true K_{d} value to be the lowest possible value of 0.1 nM, k_{off} can be estimated (with eq Error! Reference source not found., main text) to be around 10^{-4} s^{-1} . With all these considerations and eq S31, t_{eq} is calculated to be 1.4 h, and accordingly, the minimum incubation time ($3t_{\text{eq}}$) is calculated to be 4.2 h. This mathematical estimation of sufficient incubation time can save researchers time and experimental resources. However, since true k_{on} can be much smaller than $10^6 \text{ M}^{-1}\text{s}^{-1}$, ideally at least one more K_{d} -determination experiment should be conducted with a longer incubation time to confirm that $K_{\text{d,det}}$ is stabilized.

Note S10: Calibration and operations of lab balances

Laboratory mass measuring equipment, including top-loading balances, portable balances, analytical balances, semi-micro balances, and microbalances,²⁴ should be calibrated and operated meticulously. Before using a laboratory balance, it is essential to carefully read the user manual provided by the manufacturer to understand how to use and calibrate the device correctly. Regular calibration of any type of lab balance is crucial to minimize systematic errors in measured mass.²⁵

Traditionally, lab balances are manually calibrated by adjusting the balance readings using standard weights.²⁶ This manual calibration process is time-consuming and usually conducted once per month.²⁶ However, many modern lab balances now come with built-in automatic self-calibration functionality,²⁷ which offers convenience and time efficiency. Balances equipped with this function can be calibrated more often, even before every measurement.^{26, 28} It is noteworthy that the most reliable calibration for balances with self-calibration is a combination of manual and automatic calibrations.²⁶

In addition to proper calibration, users must adhere to certain rules to ensure high accuracy and precision when using a lab balance. These rules dictate:²⁹

- i) level the balance perfectly,
- ii) keep the device clean,
- iii) place the sample in a suitable container for weighing to avoid damaging the weighing pan,
- iv) tare the balance to subtract the weight of the sample container,
- v) avoid vibration and heavy airflow around the balance during weight measurement,
- vi) keep the balance away from any strong magnetic field.
- vii) maintain the balance in an environment with a stable temperature (i.e., room temperature).

Failure to comply with these rules can potentially result in significant systematic errors in measured mass.

Note S11: Calibration and operations of pipettes

The calibration of a pipette relies on the relationship between the volume and mass of distilled water aspirated/dispensed by the pipette.³⁰ Therefore, calibrating volume pipettes necessitates the use of an analytical balance that has been properly calibrated and is operated correctly, as discussed in Note S5. Pipettes are calibrated using professional tools by adjusting the readings to correspond to the volumes of distilled water aspirated and dispensed, as weighed by a highly accurate analytical balance.³⁰ This conversion between mass and volume is facilitated by the density of distilled water (volume = mass/density), which, assuming negligible effects of atmospheric pressure on water density, varies with environmental temperature.³⁰

Typically, a pipette is calibrated for both its lower- and upper-limit volumes.³¹ If the lower- and upper-limit volumes cannot be calibrated simultaneously, the pipette should not be used for volume measurement and should either be replaced or sent back to the vendor for maintenance.

When using a calibrated pipette, it is essential to adhere to the following rules to enhance the accuracy of pipetting:³²

- i) pre-wet the pipette tip at least three times before aspirating the final volume,
- ii) hold the pipette at a consistent angle not exceeding 20 degrees to the vertical,
- iii) before aspirating, immerse the pipette tip to an appropriate depth (based on the volume to aspirate/dispense) below the liquid surface to ensure contact with the liquid throughout the aspiration process,
- iv) touch off after each dispense,

v) pipette viscous liquids slowly, while pipetting volatile liquids quickly. Failure to use calibrated pipettes or to follow the aforementioned rules can result in inaccuracies in measured liquid volume.

Note S12: Avoiding reagent degradation

To avoid reagent degradation, it is crucial to store reagents under appropriate conditions and adhere to specific guidelines. For instance, for long-term storage of single-stranded DNA (ssDNA) with high concentration (> 100 ng/ μ L), the ssDNA suspension should be divided into small aliquots with small aliquots (e.g., 2 μ L) and stored at -20 °C for no longer than 2 years.³³ Repeated freeze-thaw cycles for DNA solutions should be avoided since they can lead to DNA degradation.³⁴ Additionally, long-term exposure to light, including UV light and ambient lab light, should be avoided for fluorophore-modified ssDNA to avoid photobleaching.³⁵

A working solution of ssDNA with a lower concentration can be stored in a refrigerator at $+4$ °C for one year and should be placed on ice when used to prepare samples on the bench.³⁶ Similarly, to prevent preserve proteins, solutions with high concentrations (> 1000 ng/ μ L) or lyophilized proteins should be divided into small aliquots and stored at -80 °C for long-term storage.³⁷ Repeated freeze-thaw cycles for lyophilised protein and protein solutions should also be avoided.³⁷

Due to the propensity of microorganisms to grow in protein solutions under nonfreezing conditions, working solutions of proteins with a lower concentration can only be stored at $+4$ °C for days to weeks at the longest.³⁷ Improper storage of reagents can significantly reduce the concentrations of active ligand and target molecules compromising their native structures and unavoidably introducing large systematic errors in L_0 and T_0 .

Note S13: Common measures for reducing solute adsorption

The most common and straightforward method to mitigate reagent adsorption and nonspecific binding to surfaces is by incorporating blocking reagents such as BSA protein, Tween[®] 20, and Triton X-100 into solutions. The addition of blocking agents to solutions has been proven to be an effective strategy for reducing nonspecific bindings.³⁸⁻⁴⁰

Since the extent of reagent adsorption to a surface is significantly influenced by the surface's chemical properties, instrumental parts made of adsorption-resistant materials, such as titanium and polyether ether ketone (PEEK), are preferred for use along the fluidic path.⁴¹

Furthermore, surface modification with biocompatible coatings is a widely adopted and effective approach for reducing reagent adsorption. Coatings such as Bovine Serum Albumin (BSA), Polyethylene glycol (PEG), and polyvinyl alcohol (PVA) have been shown to effectively reduce DNA and protein adsorption.⁴²⁻⁴⁴

To minimize reagent adsorption to the inner walls of vials, some manufacturers have developed various types of low-binding tubes. These tubes can be used in conjunction with other adsorption elimination methods to further mitigate reagent losses resulting from solute adsorption.⁴⁵

Table S1: Checklist for minimizing the systematic errors of variables in K_d determination with nonlinear regression

This checklist is an extended version of the checklist proposed by Jarmoskaite *et al.*²² This checklist is also stored on Figshare (DOI: 10.6084/m9.figshare.25464685) as a PDF file.

Checklist for Improving the Accuracy of Determined K_d

Ligand (limiting component): _____
Target (excess component): _____
 K_d -determination method: _____
CONDITIONS: Temperature: _____ **Buffer:** _____
Other: _____

ABBREVIATIONS AND SYMBOLS:

R , fraction of unbound ligand; ΔR , systematic error of R ; ΔK_d , systematic error of determined K_d ; $K_{d, \text{det}}$, experimentally determined K_d ; L , equilibrium concentration of ligand; L_0 , total concentration of ligand; T , equilibrium concentration of target; T_0 , total concentration of target; C , equilibrium concentration of target–ligand complex; S , measured cumulative signal S from unbound ligand and target-bound ligand; S_L^* , signal of pure ligand; S_C^* , signal of pure complex; **LOQ**, limit of quantitation; **EM**, equilibrium mixture.

Minimize ΔR (and minimize ΔK_d caused by too high L_0)	<ul style="list-style-type: none"> • Has the additivity of the signal used to calculate R been proven? Additivity of signal: $S = S_L^* \frac{L}{L_0} + S_C^* \frac{C}{L_0}$ 	<input type="checkbox"/> Yes. Continue. <input type="checkbox"/> No/Not sure. Prove the additivity or change to a different method.
	<ul style="list-style-type: none"> • Has the instrument used to detect signals been calibrated? 	<input type="checkbox"/> Yes. Continue. <input type="checkbox"/> No/Not sure. Calibrate the instrument.
	<ul style="list-style-type: none"> • Is the LOQ of the instrument for the ligand known? 	<input type="checkbox"/> Yes. Use $L_0 = \text{LOQ}$. <input type="checkbox"/> No. Measure LOQ.
	<ul style="list-style-type: none"> • Vary incubation time to confirm equilibration. Time range: _____ Number of time points: _____ <ul style="list-style-type: none"> ➤ Is $K_{d, \text{det}}$ independent to the tested incubation time? 	<input type="checkbox"/> Yes. Incubation time is sufficient. <input type="checkbox"/> No. Increase incubation time.
	<ul style="list-style-type: none"> • Does the binding isotherm “R vs T_0” reach saturation? <ul style="list-style-type: none"> ➤ <i>Check approach:</i> <ol style="list-style-type: none"> 1) Linear fit the data points of “S vs T_0” obtained from the EMs with the three highest T_0 to get a fitting equation of “$S = a + bT_0$” with slope of “$b \pm \delta b$”, i.e., uncertainty range of slope is $[b - \delta b, b + \delta b]$. 2) If $0 \in [b - \delta b, b + \delta b]$, the binding isotherm reaches saturation. Note: The highest T_0 should be at least twofold greater than the lowest T_0 in the three EMs. 	<input type="checkbox"/> Yes. Continue. <input type="checkbox"/> No. Increase the highest T_0 (if solubility allows).
Minimize ΔL_0 and ΔT_0	<ul style="list-style-type: none"> • Have the measuring instruments (e.g., balance and pipette) been calibrated? 	<input type="checkbox"/> Yes. Continue. <input type="checkbox"/> No/Not sure. Calibrate the measuring instruments.
	<ul style="list-style-type: none"> • Have the purities of ligand and target been measured with analytical approaches (e.g., HPLC and SDS-PAGE)? 	<input type="checkbox"/> Yes. Correct L_0 and T_0 based on the determined purities. <input type="checkbox"/> No. Determine the purities of ligand and target.
	<ul style="list-style-type: none"> • Are the ligand and/or target prone to adsorption to surfaces? <ul style="list-style-type: none"> ➤ <i>Common measures to reduce reagent adsorptions:</i> <ul style="list-style-type: none"> - Adding blocking agents (e.g., BAS and Tween® 20) into solutions. - Surface modifications with biocompatible coatings - Using instrumental parts and lab supplies that are made of low-binding materials. 	<input type="checkbox"/> Yes/Not sure. Apply the measures of reducing reagent adsorptions. <input type="checkbox"/> No.
Comments		

Table S2: Determination of the random error in the concentration of fluorescein (ligand) solutions

To demonstrate the determination of the random error in the concentration of fluorescein solutions, we prepared five 800 μL fluorescein stock solutions with nominal (desired) concentration of 300 μM . Each solution was prepared separately from scratch. For each sample, the absorbance at light wavelength of 488 nm (A_{488}) with path length $l = 1$ mm was measured with a NanoDrop 1000 (Thermo Scientific) spectrophotometer. The measured absorbance for each sample and the calculated relative standard deviation (RSD) are summarized here. The absorbance of each sample was measured in triplicate.

Sample #	A_{488}	Average	Overall Average	Standard Deviation (SD)	RSD ($\delta L_0/L_0$)
1	1.721	1.72	1.69	0.025	0.015
	1.708				
	1.723				
2	1.694	1.69			
	1.675				
	1.685				
3	1.648	1.67			
	1.667				
	1.684				
4	1.658	1.66			
	1.654				
	1.666				
5	1.710	1.71			
	1.702				
	1.714				

References

- (1) Maes, K.; Smolders, I.; Michotte, Y.; Van Eeckhaut, A. Strategies to reduce aspecific adsorption of peptides and proteins in liquid chromatography–mass spectrometry based bioanalyses: An overview. *Journal of Chromatography A* **2014**, *1358*, 1-13.
- (2) Weeramange, C. J.; Fairlamb, M. S.; Singh, D.; Fenton, A. W.; Swint-Kruse, L. The strengths and limitations of using biolayer interferometry to monitor equilibrium titrations of biomolecules. *Protein Science* **2020**, *29* (4), 1004-1020.
- (3) Galievsky, V. A.; Stasheuski, A. S.; Krylov, S. N. “Getting the best sensitivity from on-capillary fluorescence detection in capillary electrophoresis”—A tutorial. *Analytica Chimica Acta* **2016**, *935*, 58-81.
- (4) Jiang, L.; Xiong, Z.; Song, Y.; Lu, Y.; Chen, Y.; Schultz, J. S.; Li, J.; Liao, J. Protein–Protein Affinity Determination by Quantitative FRET Quenching. *Scientific reports* **2019**, *9* (1), 2050.
- (5) Krylova, S. M.; Dove, P. M.; Kanoatov, M.; Krylov, S. N. Slow-dissociation and slow-recombination assumptions in nonequilibrium capillary electrophoresis of equilibrium mixtures. *Analytical chemistry* **2011**, *83* (19), 7582-7585.
- (6) Kanoatov, M.; Galievsky, V. A.; Krylova, S. M.; Cherney, L. T.; Jankowski, H. K.; Krylov, S. N. Using nonequilibrium capillary electrophoresis of equilibrium mixtures (NECEEM) for simultaneous determination of concentration and equilibrium constant. *Analytical chemistry* **2015**, *87* (5), 3099-3106.
- (7) Weber, G. Polarization of the fluorescence of macromolecules. 1. Theory and experimental method. *Biochemical Journal* **1952**, *51* (2), 145.
- (8) Cottet, H.; Biron, J.-P.; Martin, M. Taylor dispersion analysis of mixtures. *Analytical chemistry* **2007**, *79* (23), 9066-9073.
- (9) Moser, M. R.; Baker, C. A. Taylor dispersion analysis in fused silica capillaries: a tutorial review. *Analytical Methods* **2021**, *13* (21), 2357-2373.
- (10) Jensen, H.; Østergaard, J. Flow induced dispersion analysis quantifies noncovalent interactions in nanoliter samples. *Journal of the American Chemical Society* **2010**, *132* (12), 4070-4071.
- (11) Clark, S. M.; Konermann, L. Determination of ligand– protein dissociation constants by electrospray mass spectrometry-based diffusion measurements. *Analytical chemistry* **2004**, *76* (23), 7077-7083.
- (12) Bielejewska, A.; Bylina, A.; Duszczuk, K.; Fiałkowski, M.; Hołyst, R. Evaluation of ligand-selector interaction from effective diffusion coefficient. *Analytical chemistry* **2010**, *82* (13), 5463-5469.
- (13) Guevara-Carrion, G.; Gaponenko, Y.; Janzen, T.; Vrabec, J.; Shevtsova, V. Diffusion in multicomponent liquids: From microscopic to macroscopic scales. *The Journal of Physical Chemistry B* **2016**, *120* (47), 12193-12210.
- (14) Barros, M. C.; Ribeiro, A. C.; Verissimo, L. M.; Leaist, D. G.; Estes, M. A. Diffusion in ternary aqueous {L-dopa+(NaSO₃) n-β-cyclodextrin} solutions using the pseudo-binary approximation. *The Journal of Chemical Thermodynamics* **2018**, *123*, 17-21.
- (15) Cussler, E. L. *Diffusion: mass transfer in fluid systems*; Cambridge university press, 2009.
- (16) Price, W. E. Theory of the Taylor dispersion technique for three-component-system diffusion measurements. *Journal of the Chemical Society, Faraday Transactions 1: Physical Chemistry in Condensed Phases* **1988**, *84* (7), 2431-2439.
- (17) Callendar, R.; Leaist, D. G. Diffusion coefficients for binary, ternary, and polydisperse solutions from peak-width analysis of Taylor dispersion profiles. *Journal of solution chemistry* **2006**, *35*, 353-379.
- (18) Leaist, D. G. Ternary diffusion coefficients of 18-crown-6 ether–KCl–water by direct least-squares analysis of Taylor dispersion measurements. *Journal of the Chemical Society, Faraday Transactions* **1991**, *87* (4), 597-601.
- (19) Rukundo, J.-L.; Le Blanc, J. Y.; Kochmann, S.; Krylov, S. N. Assessing Accuracy of an Analytical Method in silico: Application to “Accurate Constant via Transient Incomplete Separation”(ACTIS). *Analytical Chemistry* **2020**, *92* (17), 11973-11980.
- (20) Okhonin, V.; Berezovski, M. V.; Krylov, S. N. MASKE: Macroscopic approach to studying kinetics at equilibrium. *Journal of the American Chemical Society* **2010**, *132* (20), 7062-7068.

- (21) Olson, S. T.; Srinivasan, K.; Björk, I.; Shore, J. D. Binding of high affinity heparin to antithrombin III. Stopped flow kinetic studies of the binding interaction. *Journal of Biological Chemistry* **1981**, 256 (21), 11073-11079.
- (22) Jarmoskaite, I.; AlSadhan, I.; Vaidyanathan, P. P.; Herschlag, D. How to measure and evaluate binding affinities. *Elife* **2020**, 9, e57264.
- (23) Schreiber, G.; Haran, G.; Zhou, H. X. Fundamental aspects of protein-protein association kinetics. *Chem Rev* **2009**, 109 (3), 839-860. DOI: 10.1021/cr800373w From NLM.
- (24) *How Laboratory Scales Work & How Leasing Benefits Labs.* excedr, 2024. <https://www.excedr.com/general-lab-equipment/lab-balance> (accessed 2024 03-18).
- (25) General Chapter 41 "Balances". In *U.S. Pharmacopeia*, USP - NF, 2021.
- (26) O'Driscoll, A. *A Guide to Balance and Scale Calibration*. Laboratory Supply Network, Inc., 2018. <https://labbalances.net/blogs/blog/balance-and-scale-calibration-guide> (accessed 2024 03-20).
- (27) *Analytical Balances with Internal Calibration*. METTLER TOLEDO, 2024. [https://www.mt.com/us/en/home/products/Laboratory_Weighing_Solutions/analytical-balances/analytical-balances-with-internal-calibration.html?filter\[balance-line\]=ML-T&filter\[balance-line\]=XPR](https://www.mt.com/us/en/home/products/Laboratory_Weighing_Solutions/analytical-balances/analytical-balances-with-internal-calibration.html?filter[balance-line]=ML-T&filter[balance-line]=XPR) (accessed 2024 03-18).
- (28) Kogut, A. *How to Use Internal Calibration on Your Weighing Scale or Balance*. Inscale Ltd, 2023. <https://www.inscale-scales.co.uk/blogs/weighing-scales-blog/how-to-use-internal-calibration-on-your-weighing-scale-or-balance> (accessed 2024 03-22).
- (29) French, L. *The Do's and Don'ts of Laboratory Balances*. Labcompare, 2023. <https://www.labcompare.com/10-Featured-Articles/596136-The-Do-s-and-Don-ts-of-Laboratory-Balances/> (accessed 2024 03-18).
- (30) Saha, S. *Performing Pipette Calibration Yourself*. Bitesize Bio, 2021. <https://bitesizebio.com/40766/performing-pipette-calibration-yourself/> (accessed 2024 03-18).
- (31) Juncker, M. *How to Do Pipette Calibration*. wikiHow, Inc., 2024. <https://www.wikihow.com/Do-Pipette-Calibration> (accessed 2024 03-20).
- (32) *10 Steps to Improve Pipetting Accuracy*. Thermo Fisher Scientific 2024. <https://www.thermofisher.com/ca/en/home/life-science/lab-plasticware-supplies/lab-plasticware-supplies-learning-center/lab-plasticware-supplies-resource-library/fundamentals-of-pipetting/proper-pipetting-techniques/10-steps-to-improve-pipetting-accuracy.html> (accessed 2024 03-18).
- (33) Chkaiban, L.; Tosi, L.; Parekkadan, B. Assembly of Long-Adapter Single-Strand Oligonucleotide (LASSO) Probes for Massively Parallel Capture of Kilobase Size DNA Targets. *Curr Protoc* **2021**, 1 (11), e278. DOI: 10.1002/cpz1.278 From NLM.
- (34) Shao, W.; Khin, S.; Kopp, W. C. Characterization of effect of repeated freeze and thaw cycles on stability of genomic DNA using pulsed field gel electrophoresis. *Biopreserv Biobank* **2012**, 10 (1), 4-11. DOI: 10.1089/bio.2011.0016 From NLM.
- (35) Wagner, E. *My oligos have arrived: Now what?* Integrated DNA Technologies, Inc., 2014. <https://www.idtdna.com/pages/education/decoded/article/my-oligos-have-arrived-now-what-> (accessed 2024 03-20).
- (36) Speicher, N. P. N. *Storing oligos: 7 things you should know*. Integrated DNA Technologies, Inc., 2017. <https://www.idtdna.com/pages/education/decoded/article/storing-oligos-7-things-you-should-know> (accessed 2024 03-20).
- (37) *Protein stability and storage*. Pierce Biotechnology, Inc., 2003. https://wolfson.huji.ac.il/purification/PDF/StorageProteins/PIERCE_ProteinStorage.pdf (accessed 2024 03-20).
- (38) Batteiger, B.; Jones, R. B. The use of Tween 20 as a blocking agent in the immunological detection of proteins transferred to nitrocellulose membranes. *Journal of immunological methods* **1982**, 55 (3), 297-307.
- (39) Esser, P. *Blocking Agent and Detergent in ELISA* Thermo Fisher Scientific Inc. , 2014. <https://assets.fishersci.com/TFS-Assets/LSG/Application-Notes/D19564.pdf> (accessed 2024 03-20).

- (40) Osumi, K.; Ozeki, Y.; Saito, S.; Nagamura, Y.; Ito, H.; Kimura, Y.; Ogura, H.; Nomura, S. Development and assessment of enzyme immunoassay for platelet-derived microparticles. *Thrombosis and haemostasis* **2001**, 85 (02), 326-330.
- (41) Guimaraes, G. J.; Bartlett, M. G. Managing nonspecific adsorption to liquid chromatography hardware: A review. *Analytica Chimica Acta* **2023**, 1250, 340994.
- (42) Auvinen, H.; Zhang, H.; Nonappa; Kopilow, A.; Niemelä, E. H.; Nummelin, S.; Correia, A.; Santos, H. A.; Linko, V.; Kostianen, M. A. Protein Coating of DNA Nanostructures for Enhanced Stability and Immunocompatibility. *Adv Healthc Mater* **2017**, 6 (18). DOI: 10.1002/adhm.201700692 From NLM.
- (43) Zhang, X.; Huang, P.-J. J.; Servos, M. R.; Liu, J. Effects of Polyethylene Glycol on DNA Adsorption and Hybridization on Gold Nanoparticles and Graphene Oxide. *Langmuir* **2012**, 28 (40), 14330-14337. DOI: 10.1021/la302799s.
- (44) Barrett, D. A.; Hartshome, M. S.; Hussain, M. A.; Shaw, P. N.; Davies, M. C. Resistance to nonspecific protein adsorption by poly(vinyl alcohol) thin films adsorbed to a poly(styrene) support matrix studied using surface plasmon resonance. *Anal Chem* **2001**, 73 (21), 5232-5239. DOI: 10.1021/ac010368u From NLM.
- (45) Grzeskowiak¹, R.; Hamels, S.; Gancarek, E. Comparative Analysis of Protein Recovery Rates in Eppendorf LoBind® and Other “Low Binding” Tubes. *AG Application Note* **2016**.